Spring 2021

Predictions of Knee Joint Contact Forces Using Only Kinematic Inputs with a Recurrent Neural Network

Kaileigh Elisabeth Estler
Old Dominion University, kaileighelisabeth1@gmail.xom

PREDICTIONS OF KNEE JOINT CONTACT FORCES USING ONLY KINEMATIC INPUTS WITH A RECURRENT NEURAL NETWORK

By

Kaileigh Elisabeth Estler
B.S. May 2019, Old Dominion University

A Thesis Submitted to the Faculty of
Old Dominion University in Partial Fulfillment of the
Requirements for the Degree of

MASTER SCIENCE IN EDUCATION
EXERCISE SCIENCE

OLD DOMINION UNIVERSITY
May 2021

Approved by:

Hunter J. Bennett (Chair)

Rumit Singh Kakar (Member)

Stacie Ringleb (Member)

Kevin Valenzuela (Member)

ABSTRACT

PREDICTIONS OF KNEE JOINT CONTACT FORCES USING ONLY KINEMATIC INPUTS WITH A RECURRENT NEURAL NETWORK

Kaileigh Elisabeth Estler
Old Dominion University, 2021
Director: Dr. Hunter J. Bennett

BACKGROUND: Knee joint contact (bone on bone) forces are commonly estimated using surrogate measures such as external knee adduction moments (with limited success) or musculoskeletal modeling (more successful). Despite its capabilities, modeling is not optimal for clinicians or persons with limited experience and knowledge. Therefore, the purpose of this study was to design a novel prediction method for knee joint contact forces that is equal or more accurate than modeling, yet simplistic in terms of required inputs. METHODS: This study included all six subjects' (71.3±6.5kg, 1.7±0.1m) data from the opensource "Grand Challenge" datasets (simtk.org) and two subjects from the "CAMS" datasets, consisting of motion capture and in-vivo instrumented knee prosthesis data (e.g. true knee joint contact forces). Inverse kinematics were used to derive three-dimensional hip, two-dimensional knee (sagittal & frontal), and one-dimensional ankle (sagittal) kinematics during the stance phase of normal walking for all subjects. Medial and lateral knee joint contact forces (normalized to body weight) and inverse kinematics were imported into MATLAB and normalized to 101 data points. A long-short term memory network (LSTM) was created to predict knee forces using combinations of the kinematics inputs. The Grand Challenge data were used for training, while the CAMS data were used for testing. Waveform accuracy was explained by the proportion of variance and root mean square error between network predictions and in-vivo knee joint contact forces data.
RESULTS: The top five networks demonstrated excellent fit with the training data, achieving RMSE < 0.26BW for medial and lateral forces, R^2 > 0.69 for medial forces, but only R^2 > 0.15

for lateral forces. The overall best-selected network contained frontal hip and knee, and sagittal hip and ankle input variables and presented the finest visual waveform agreement with the in-vivo data (R^2=0.77, RMSE=0.27). CONCLUSIONS: The LSTM network designed in this study revealed knee joint forces could accurately be predicted by using only kinematic input variables. The network's results outperformed most reports of root mean squared errors and correlation coefficients attained by musculoskeletal modeling and surrogate measures of KAMs.

TABLE OF CONTENTS

TABLE OF TABLES

TABLE OF FIGURES

CHAPTER I
INTRODUCTION

The purpose of this study is to examine the non-linear relationship between the biomechanical (kinetic and kinematic) factors that attribute to in-vivo knee joint data. Currently, in-vivo knee joint contact forces (KJCF) are measured by instrumented implant technology in persons with total knee replacements (TKR). Although this method is not necessarily indicative of all populations, research using in-vivo data, albeit limited in sample size, has illuminated the intricate relationship between experimentally measured dynamics and bone-on-bone forces. Recent advancements in musculoskeletal modeling have allowed for quite accurate estimates of KJCF without the limitation/requirement of TKR instrumentation, thus making results more generalizable to the population at large. However, the required comprehensive skills for modeling is quite complex and lacks practicality for many researchers and clinicians. For this reason, an efficient surrogate method of KJCF is by the external knee adduction moment (KAM). Computation of the KAM requires input from both kinematic measures (i.e. joint angles) and ground reaction forces (GRFs), typically obtained using three-dimensional motion capture systems. However, as the following literature review will demonstrate, alterations of the KAM, which is a typical goal of gait training studies that regard knee health, occurs primarily through modifications of the joint kinematics and not GRFs. Thus, kinematic measures could be an efficient alternative predictor for KJCF that are more easily attained, require less computations, and are relevant to both researchers and clinicians alike.

The following literature review (Chapter II) will 1) review the common methods for measuring and predicting in-vivo KJCF, 2) explain the non-linear relationship between surrogate kinematic measures and kinetics to predict KJCF, and 3) introduce an artificial recurrent neural network as a means of predicting KJCF with derived KJ data.

STATEMENT OF PROBLEM

True in-vivo KJCF data are currently measured by instrumented implantation technology in populations with TKR. However, instrumented implant data are scarce. Thus, focus has shifted towards musculoskeletal model simulations and surrogate measures, such as KAM, as alternative methodologies to estimate KJCF. However, despite the fact that previously literature demonstrates kinematics (i.e. movement patterns) play an integral role in KJCF, no studies have investigated the possibility of utilizing kinematic data to predict in-vivo joint forces.

PURPOSE

Knee joint contact forces (bone on bone forces) are commonly sought in biomechanics via complex musculoskeletal modeling or estimated using surrogate measures such as external KAMs. However, musculoskeletal modeling is not optimal for clinicians or persons with limited experience pertaining to modeling and KAMs have been found ineffective at predicting KJCF during altered gait patterns (i.e. non-normal). As such, it is pertinent to devise a new prediction methodology that arises from as few experimental technologies as possible and is not bound to the complexity of modeling. Therefore, the purpose of this study is to design a recurrent neural network to predict knee joint contact forces using input variables of only kinematic measures.

SIGNIFICANCE OF STUDY

This study will provide new insight for predicting in-vivo KJ data from a more widely applicable approach. Current methodologies are limited by the accessibility of implanted instrumented in-vivo data and the high level of knowledge necessary for musculoskeletal modeling. Not only is the aim of this work to develop a better method for predicting in-vivo data, but to also demonstrate the relationship between kinematic parameters and KJCF.

HYPOTHESIS

Hypothesis 1 – A recurrent neural network consisting of only kinematic inputs can predict KJCF with higher accuracy levels matching those reported using musculoskeletal modeling.

Hypothesis 2 – More than one combination of kinematic variables can match the level of accuracy reported using musculoskeletal modeling.

LIMITATIONS

- This study, and thus the neural network, will include only data from opensource databases of persons who have had an instrumented TKR, which is a very limited subject pool. To date, there are only two widely available data: Grand Challenge Competition (simtk.org; 6 datasets, two repeated subjects, JW & DM) and CAMS-Knee (single trial from two subjects K5R & K8L, https://CAMS-Knee.orthoload.com, Taylor et al. 2017).
- Not all subjects had the same knee replacement instrumentation or force transducers. However, calculations for the medial and lateral KJCF were validated for each force transducer via mechanical testing. The variation in instrumentation among subjects should allow the neural network to perform more generalizable predictions.
- This study will not include data from otherwise healthy individuals, thus limiting the generalizability of the results. However, unlike musculoskeletal models, this study will only include kinematic variables, which should be more generalizable than vast computational models including predicted muscle activation and contraction dynamics.

DELIMITATIONS

- Kinematic variables included in the neural network will be limited to those of the lower extremity (3-hip, 2-knee, and 1-ankle) and trunk sway.
- Artificial neural networks can be trained with seemingly an infinite number of neurons. However, the range of neurons that will be included in the network here will be limited from 5-20 neurons.
- This study will focus on predicting medial and lateral knee joint compartment forces. Although it is possible to train a network to predict all 6-components of in-vivo KJCF, the computational requirements would be likely to require more subject data than available.

OPERATIONAL DEFINITIONS

Knee joint contact forces (KJCF): the true bone on bone forces between the distal femur and proximal tibia

Knee osteoarthritis (KOA): the degradation of meniscus cartilage at the knee joint, often leading to extreme pain and discomfort

Instrumented implanted in-vivo data: biomechanical data collected from a technological device post knee arthroplasty/replacement

Total knee replacement (TKR): surgical procedure to remove degenerated cartilage and bone at the KJ

CHAPTER II

LITERATURE REVIEW

Mobilization and stability are the primary roles of the knee joint, aided by its surrounding soft tissues that absorb and convey the stress demands placed on the body throughout all planes of movement (Neumann, 2002). Consequently, the subjective continuous breakdown of cartilage is one of the leading causes of joint disease and disorder, known as osteoarthritis (OA) (Kremers et al., 2015). Factors such as age and repetitive use of the KJ contribute to the prevalence of OA. Physical burdens associated with OA are categorized by unbearable pain, increased stiffness or decrease in range of motion (ROM), and swelling at the KJ (Bade et al., 2010). Though there is no direct cure for OA, patients can undergo procedural total knee replacement (TKR) to manage the excruciating signs and symptoms. The objective of TKR operations is to improve functional daily living and alleviate the pain associated with OA (Ko et al., 2011). Although the exact number of KJ procedures among the United States population is unknown, in 2010 it was estimated that 4.7 million individuals have undergone TKR surgeries (Kremers et al., 2015). That is, about 4% of adults over 50 years live with TKR (Weinstein et al., 2013; Kremers et al., 2015). Expected growth in TKR demand is rising amongst the younger population (Hootman & Helmick, 2006), and so it is pertinent to investigate the effectiveness of current TKR procedures in correlation with previous biomechanics research. The primary goal of knee replacement is to restore mechanical function and efficiency at the KJ. Investigating the habitual kinematic and dynamic patterns (joint loads and knee angles) of the KJ can provide insight into individuals' mechanical in-vivo gait patterns.

Subjective questionnaires are often utilized to survey patient satisfaction post TKR. Overall, about 81% of TKR patients have reported complete procedural satisfaction, thus indicating a significant portion of patients that fall on the opposite end of satisfaction (Bourne et al., 2010). The majority of dissatisfied patients were of the older age margin, 61-74 years (Noble et al., 2006). Bourne et al., (2010) assessed KJ stiffness post-operation and reported the activities experienced at the lowest satisfactory level were walking up and down the stairs and getting out of automobiles. For this reason, comparisons of KJ patterns (i.e. kinematics and kinetics) in clinical populations (KOA) versus healthy persons are an important step in ascertaining the mechanisms driving satisfaction/success with TKR.

In both laboratory and clinical settings, procedural 3-dimensional motion capture analysis can be implemented to measure kinematic and kinetic variables. Inverse dynamic analyses allow researchers to calculate the net (minimum necessary) force and moments during activities such as walking. In OA patients there is an increased dynamic load (i.e. forces and moments) at the KJ as the degenerative disease progresses. During dynamic assessments such as gait, the knee adduction moment (KAM) exhibits the greatest moment arm magnitude, respective to the knee (Felson, 2003). The KAM is also believed to be the optimal predictor of knee OA (KOA) progression due to the repetitive overload at the medial compartment of the knee (Walter et al., 2010; Zhao et al., 2006).

Other equally important factors that influence KJCF patterns during gait are alignment and kinematic gait patterns both before and after TKR operations (Noble et al., 2006; Vissers et al., 2010). Tibiofemoral malalignments expressed as varus (mechanical axis <0°) and valgus (mechanical axis>0°) are often indicative of insufficient load distribution in the medial and lateral distributions. Most commonly, varus alignment is often associated with greater medial compartmental loading at the KJ in KOA populations compared to neutral and valgus alignments and is expressed by peaks of KAM (Nie et al., 2019; Turcot et al., 2013; Simic et al., 2013;

Messier et al., 2014). To compensate for altered gait kinetics and kinematics in the knee driven by tibiofemoral malalignment, corrective osteotomies are considered. In an attempt to correct valgus alignment and the high lateral load demand, slight varus/neutral osteotomies were evaluated in patients with lateral KOA (Egmond et al., 2017). As expected, peaks of KAM significantly increased, thus reducing the pre-operative lateral compartment load and KOA progression (Egmond et al., 2017). Although the KOA group still had less sagittal ROM post-op primarily at toe-strike and heel-off, the corrective alignment successfully resembled the controls' gait patterns (Egmond et al., 2017).

Inverse dynamics research has shed light on the altered/abnormal gait mechanics of persons with KOA and/or a TKR. However, inverse dynamics is only a surrogate measure of the true target, KJCF. Therefore, it is important to discuss the methods in-vivo KJCF have been previously recorded via advanced technology.

MEASURING IN-VIVO KJ FORCES VIA INSTUMENTED IMPLANT TECHNOLOGY

With recent advancements in technology, knee joint contact forces (the true bone on bone forces between the distal femur and proximal tibia) can be recorded in-vivo during a variety of activities (Geffre et al., 2007; Szivek et al., 2006). The methodology "instrumentation" is designed to replicate the function of knee cartilage using a scaffold of engineered tissue in patients with OA and simultaneously measure in-vivo joint loads via implanted force-plate data (Geffre et al., 2007; Szivek et al., 2006). Further research has advanced in creating multi-dimensional devices to measure the six force components (F_x, F_y, F_z, T_x, T_y, T_z) that act on the tibiofemoral contact points during dynamic tests (Kirking et al., 2006). This instrumented design has been shown to objectively measure static and dynamic force components via sensor plate information (Geffre et al., 2007). A total of seven out of nine sensor plate implants among three canines revealed this method to be a successful means of measuring KJ force data relative to TKR progress (Geffre et al., 2007).

Throughout activities of daily living (ADL) the knee undergoes repeated bouts of stress under all components. The typical load range acting at the KJ during the majority of ADL yields 220-350% BW (Kutzner et al., 2010). To evaluate the functional success of an 81-year-old male post knee implantation surgery, in-vivo data was collected during several ADLs (Mündermann et al., 2008). Peak KJ compressive loads during the ascending and descending phase of stair walking yielded a magnitude load of 2.5x the participants' body weight (64.5kg) (Mündermann et al., 2008). In a similar study, one 80-year-old participant presented a peak tibial force during walking when the load was 2.2 times greater than their body weight (D'Lima et al., 2006). In-vivo data of medial versus lateral knee compartmental load distribution ratios exhibited greater load magnitudes at the medial compartment during several ADL (Mündermann et al., 2008; Zhao et al., 2006). The medial compartment endured greater force loads during squats and chair-sit to stand, 2.7 and 2.2 times greater than body weight (BW), respectively (Mündermann et al., 2008). Similar results were obtained by in-vivo data during level gait walking and step-up/step-down exercises (Zhao et al., 2006). During level walking the peak medial load over total load was 53% and 56% during step-up/step-down, thus resembling the expected TKR gait patterns with a greater medial KJ compartment load distribution (Zhao et al., 2006). A note of caution is due here, as the majority of studies measuring in-vivo KJ forces via instrumented implantations are limited by single subject participants. However, Kutzner et al. (2010) analyzed in-vivo KJ data among 5 participants, each with a 6-load tibial plate implantation. Consistent with previous findings, the average peak resultant force was greatest during stair ascent (316%BW) and descend (346%BW) (Kutzner et al., 2010; Mündermann et al., 2008; Heinlein et al., 2009).

In-vivo KJ moments displayed the greatest magnitudes about the frontal plane during all activities (Kutzner et al., 2010; Heinlein et al., 2009). Among two individuals with instrumented knee implants, both recorded maximum frontal plane moments during stair descending (-3.3 and -4.6%BW*m), thus indicating a greater load by the knee adduction moment (KAM) (Heinlein et al., 2009). Similarly, observed increases in frontal moments at the KJ were consistent during high knee flexion activities (Kutzner et al., 2010). The reported findings could be attributed to the higher demand on the medial knee compartment (Kutzner et al., 2010).

Overall, the findings present relative success in terms of measuring in-vivo joint forces by implantation; however, there are limitations with the small sample sizes. Despite the limited literature on this particular topic, the studies presented thus far highlight the need to understand load magnitudes during several ADL for improving implantation design (Mündermann et al., 2008; Kutzner et al., 2010). Although this is illustrated as the gold technique to measure true in-vivo joint data of all force components, the limited availability of instrumented implant technology diminishes the application to all population ranges. It is also indicated that this method is not only limited by accessibility but time and cost. Therefore, it is important to consider additional factors that contribute to KJ load distributions and joint contact forces with the ability to do so on a more subject-specific basis. Further studies, which take these variables (i.e. joint alignment, muscle group strength) into account as surrogate measures of predicting KJCF to improve knee implant instrumentation often utilize model simulation skills and procedures. As a consequence of the limited persons with instrumented knee implants, musculoskeletal modeling/simulation is currently one of the most accurate methods for predicting in-vivo KJ force data.

MODELING & SIMULATIONS TO PREDICT KJ FORCES

The utilization of model simulation techniques is thought to be “the next best thing” in terms of predicting in-vivo contact forces (Knarr & Higginson, 2015). In fact, many research groups have found a high level of success predicting in-vivo measures from instrumented TKRs, with root mean squared errors less than 0.3 bodyweights and correlation coefficients above 0.8 (Jung et al., 2016; Chen et al., 2014; Lerner et al., 2015). In addition, the “Grand Challenge Competition in Knee to Predict In Vivo Knee Loads” was specifically created to 1) garner attention and focus from the modeling/simulation community and 2) provide opensource datasets for validating user-created models.

Comparisons of predicted and in-vivo data for an 83-year-old male subject with a TKR revealed that the predicted simulated joint forces exhibited greater peak force values than the in-vivo measures during gait walking trials (Ding et al., 2016). However, modeling complexity can partially explain variability in the accuracy of predicting joint contact forces (Hast & Piazza, 2013; Kia et al., 2014). In subject-specific models, confounding factors of accurate measures of medial and lateral KJ load distribution were attributed by the generic parameters necessary for gait-models (muscle lengths, tendon compliance, activation dynamics, muscle force-velocity, and force-length) (Kia et al., 2014). Whereas subject-specific models can be customized by altered parameters such as frontal plane knee alignment, knee joint contact point location, anthropometrics, muscle activation and strength, and ligaments. Comparisons of blinded and unblinded models during walking gait trials were analyzed with instrumented in-vivo data in an

83-year male TKR patient (Smith et al., 2010). The unblinded model was designed with skeletal geometries specific to the subject, and after inverse dynamics and static optimization, the models' predicted medial, lateral, and total forces were agreeable with the instrumented TKR data (RMS = 0.23, 0.22, 0.33) (Smith et al., 2016).

In a similar study, a general model with 19 segments and 18 tri-axis hinge joints was a scaled and customized model to be compared with instrumented in-vivo experimental data during walking gait trials (Kia et al., 2014). Although comparison of the model and experimental data were presented as accurate and agreeable for kinematic loads, there were some discrepancies specific to the model-based gait cycle patterns (Kia et al., 2014). The underestimated anterior-posterior force during the gait cycle may be limited by the models' inability to predict muscle co-contractions respective to toe-off and push-off of the contralateral limb (Kia et al., 2014). This indicates that utilizing a subject-specific model kinematics can better predict in-vivo joint contact forces.

However, Hast and Piazza (2013) argue that measured contact force errors observed in model simulation techniques will decrease as more subject-specific models are developed and implemented. Although that may be the case, the demanding challenge in creating a wide range of applicable subject-specific models efficiently does not outweigh the benefits presented by this technique. In fact, Kia et al., (2014) argue that in order to attain subject-specific parameters prescribed MRIs would be highly recommended to predict muscle attachment sites.

Overall, the objective of utilizing model simulation techniques to predict in-vivo contact forces is a practical skill among biomechanists; however, the complexity presented in this approach is restrictive to those with that specific training experience. This method of analysis has several limitations, with specific regard to the essential knowledge required for repeatedly building subject-specific models. Therefore, it is justified to investigate supplementary methods of predicting joint contact forces that could be utilized in clinical settings

EXPERIMENTAL DATA COMPARING POPULATIONS AS MEASUREMENTS OF KJ DATA

Although model simulation techniques is thought to be the best methodology for predicting KJCF, the previous section presents major weaknesses. Considering that, it is sensible to find the relationship between in-vivo data with kinematics and kinetics factors to be able to predict KJCF. The comparison of clinical and healthy KJ data is an appropriate method to present the connection between kinematic and kinetic data as a means of predicting KJCF. There has been a focus on the prominent kinetic and kinematic variables on joint loads among KOA and control groups (Messeir et al., 2014; Astephen et al., 2007). Experimental data from both healthy and clinical populations is often analyzed with comparisons to instrumented in-vivo data and model simulation data. Measured joint angles and moment magnitudes are utilized as surrogate measures to predict KJCF.

Persons with KOA have demonstrated slower walking times compared to the healthy control group (Kumar et al., 2013). Overall, the OA group walked at slower walking speeds and recorded greater varus alignment (M=6.4˚) with respect to controls' alignment (M=1.2˚), measured by radiographic assessment (Kumar et al., 2013). Specifically, in persons with KOA, frontal loading magnitudes are surrogate measures to predict forces at the KJ (Favre et al., 2012; Hunt et al., 2011; Richards et al., 2018). During normal modeled gait, the peak medial KJ contact forces were associated with the 1st peak of KAM and KFM (R^2=0.73) (Richards et al., 2018). The relationship between KAM 1st peak and medial KJ contact force also had a strong association (R^2=0.83) (Richards et al., 2018).

Persons classified with more severe KOA demonstrate greater extended knee position at initial contact during walking at self-selected speeds (Mündermann et al., 2005). During the gait cycle, the stance phase contributes to about 60% of stride in the normal and healthy individual; however, KOA patients spend more time in the stance phase, specifically at double limb support (Hálfdanardóttir et al., 2018). This is indicative of a prolonged gait cycle and a decreased walking cadence at 120-130 steps/min respective to healthy adults at 100-110 steps/min (Sparkes et al., 2019). As KOA progresses, greater magnitudes of stress are placed on the KJ and consequently impact gait timing and patterns.

In comparison to healthy normal individuals, those with KOA exhibit larger magnitudes of 1st peak KAM at the early stance phase of walking, indicating a greater magnitude of medial compartment loading stress and progresses the degradation of knee cartilage (Hunt et al., 2006; Hurwitz et al., 2002). Peaks of KAM generally increase with KOA severity and so characterize the progression of the degenerative disease at the KJ (Sparkes et al., 2019; Bennell et al., 2011; Nie et al., 2019). For instance, MRI images of medial KOA were obtained and analyzed with baseline measurements of the 1st KAM peak magnitudes and KAM impulse that were recorded via 3-D gait analysis (Bennell et al., 2011). The final results showed a greater relationship between increased loss of cartilage over 12 months and a higher KAM impulse magnitude at baseline, rather than KAM peak (Bennell et al., 2011). This observation illustrates the negative consequence of a greater instant load at the KJ and its influence on cartilage degradation. Comparable results found both the peak of KAM and KAM impulse to be positively associated with medial tibiofemoral cartilage defects apparent in KOA, thus indicating individuals' predisposing factors do contribute to the magnitudes of KJ contact forces and loads (Creaby et al., 2010).

Two groups with KOA exhibited a greater KAM peak at midstance and a reduced KFM at stance compared to those reported as KOA asymptomatic; however, just one group reported a higher KFM peak at the late stance phase of walking (Astephen et al., 2007). Interestingly, KOA patients both with and without TKR exhibited greater peaks of KAM at mid-stance during walking and with concurrently reduced peak knee flexion compared to asymptomatic patients (Astephen et al., 2007). Throughout the literature, greater magnitudes of KAM peaks are consistently observed among those with KOA. However, there are disparities when reporting knee flexion moments (KFM) (Kumar et al., 2013; Mündermann et al., 2005; Sparkes et al., 2019). In persons with medial KOA, there was a statistically weak association of KFM as a predictor of medial KJCF, whereas KAM showed a greater statistical association (Richards et al., 2018). However, KFM magnitudes factored a greater influence on KJCF at initial degradation of KOA, whereas KAM is then presented to be the stronger contributor as structural degradation progresses at the KJ (Meireles et al., 2016). Overall, the inconsistent findings that pertain to KFM may also be in part due to the insufficient literature that focuses on the influence of KFM in populations with KOA.

Although KAM is generally a successful surrogate measure for KJCF, in contrast to previous research, Messier et al. (2005) did not find a significant correlation between knee joint forces and moments among standardized OA and healthy matching participants nor were reductions in KAMs coincident with reductions in-vivo medial KJCFs during gait modifications (Walter et al. 2010). As such, it is important to consider alternative measures, specifically focusing on those that are influential to the KAM and KFM (e.g. kinematics and ground reaction forces).

ALTERNATIVE MEASUREMENTS

Although KAM is noted to be an appropriate surrogate measure of KJCF, it is also necessary to understand the influential factor of lower extremity kinematics and GRFs. The characteristics related to peaks of KAM are strongly related to the orientation of the knee joint and the GRF magnitudes in the frontal plane (Hunt et al., 2006; Shull et al., 2013).

In an attempt to decrease the extensive medial compartmental load, particular gait modifications such as altered foot progression angles (FPA) have been widely considered by recognizing the corresponding shift in GRF towards the center of the KJ (Guo et al., 2007; Simic et al., 2013; Khan et al., 2017). Several studies have found gait modifications of toe-in walking reduced KAM peaks, specifically at early stance (Simic et al., 2013; Shull et al., 2013; Paquette et al., 2015). A significant reduction in the 1st peak of KAM was observed in those with medial compartment knee OA compared to healthy individuals during toe-in altered gait (Shull et al., 2013). The altered moment arms successfully reduced peak KAM exclusive of no change in peak GRF magnitude (Shull et al., 2013). Toe-in FPA has been reported successful in reducing 1st peaks of KAM during walking; however, its impact on 2nd KAM peaks is still uncertain (Simic et al., 2013). Both 2nd peak KAM and KAM impulse have been exhibited insignificant changes with toe-in gait modifications (22.3% and 5.7%) (Simic et al., 2013). On the other hand, coupling toe-in gait with wide step corrections has shown success in reducing both peaks of KAM during stair ascent (Bennett et al., 2016). Similarly, modified toe-out gait significantly reduced the 2nd peak of KAM during walking (1.3%BWxHT) and stair ascent (2.31%BWxHT) in patients with medial compartment KOA (Guo et al., 2007). Overall, adopting tailored gait patterns to correct inadequate KJ load distributions exhibited by individuals with OA can be a practical and effective method. What is important to point out here, is the conspicuous relationship between observed kinematic patterns and KJCF. For this reason, further research is warranted to demonstrate the advantages of utilizing just kinematic variables to predict in-vivo KJ data.

Modifications in toe angle during gait should not only improve joint load but also reduce the magnitude of experienced pain in those with knee OA (Simic et al., 2013). Expected outcomes may be advanced by implementing biomechanic analyses specific to individual kinematic data, prior to TKR procedures. For example, tibiofemoral and patella alignment have been found to influence frontal plane joint loading, as measured by KAM peak magnitudes (Messier et al., 2014). In clinically obese KOA individuals, BMI and patellofemoral (PF) alignment were revealed independently of one another during walking gait trials (Messier et al., 2014). Frontal plane loading expressed the imbalance of shear forces in which varus alignment displayed greater KAM peaks respective to a valgus and neutral alignment, whereas total compressive PF force was significantly influenced by BMI (Messier et al., 2014). The influence of mechanical axis alignment has been investigated with regards to load distribution in both sagittal and frontal planes at the KJ. The observed relationship between varus alignment in KOA patients has been shown to have greater medial load distributions, as demonstrated by peaks of KAM. Considering this, previous literature has evaluated the influence of patellofemoral alignment characterized by gait mechanics in both clinical and healthy populations.

Similarly, trunk sway has been implemented in an attempt to reduce the load at the medial knee compartment using the KAM surrougate measure (Mündermann et al., 2008; Kinney et al., 2012; Hálfdanardóttir et al., 2020; Walter et al., 2010; Van Den Noort et al., 2013). With this respect, it is important to note that KAM is a product of its mechanical axis and GRF (Hunt et al., 2005). Increasing mediolateral trunk sway during walking decreases frontal hip and knee moments by shifting the center of mass, and thus the resulting GRF, away from the affected knee. However, with that positive alteration, sagittal knee angle, a negative result, increased at heel-strike (Mündermann et al., 2008). This finding demonstrates the complex multi-planar relationship of kinematics with kinetics. The relationship displayed by altered dynamic alignment and a change in magnitudes of KAM peaks thus demonstrate the important role of both attributing factors to measuring and predicting in-vivo KJ data. As the prevalence of TKR procedures continues to rise, there is an increased demand for pre-procedural evaluations and accessibility. For these reasons, further research should investigate the implications of utilizing kinematics to predict in-vivo joint data as a means to bypass the current limitations and complications previously discussed.

SUPPORT FOR KINEMATIC & GRF PREDICTOR VARIABLES FOR KJ FORCE

Overall, each method discussed in contribution to predicting in-vivo KJ forces has manifested kinematics as a primary aspect; ergo, implementing kinematic analyses to predict KJCF would be highly beneficial from both research and clinical aspects. Kinematic gait analyses indicated deficits in knee flexion angles and hip moments when walking, thus limiting KJ function post-surgery (Mizner & Snyder-Mackler, 2005). From the results of altered plane kinematics, it is clear that kinematic data may provide the most practical, advantageous contribution in predicting in-vivo forces. Additionally, utilizing individual kinematic data may improve predictions of patient satisfaction in those with progressive knee OA.

MEASURES TO PREDICT IN-VIVO KJCF

The task to predict in-vivo KJCF with just kinematic parameters could be undertaken by using machine learning (ML). However, the linear algorithm processed in basic ML is limiting for complex data sets. To compensate for this boundary, a specific division of ML known as deep learning (DL), utilizes techniques for efficient data feature extraction and selection with simultaneous classification. Types of DL neural networks include artificial (ANN), convolutional (CNN), and recurrent (RNN). Each neural network is made up of three components: the input layer, the hidden layer(s), and the output layer. Both ANN and CNN models are suitable for data sets of imaging by way of a feed-forward mechanism. Current biomechanics research has utilized neural networks for image indexing purposes (Du et al., 2017; Nelson et al., 2019; Fragkiadaki et al., 2015). Specifically, in KOA populations, experimental MRI data were used as input to predict disease progression (Du et al., 2018). The best performance was achieved by an ANN model with an area under the curve ranging from 0.695-0.785, and an F-measure of 0.743-0.796 (Du et al., 2018).

Neural network applications have also been used to predict KJ forces based on measured kinematics (Favre et al., 2012; Liu et al., 2009; Arjmand et al., 2013). A strong correlation is presented between predicted KAM curves and inverse kinematics in KOA gait trials (r=0.966) (Favre et al., 2012). Strong trends continue to be presented by the hip, knee, and ankle moments predicted by ANN, all associations greater than 0.95 during walking gait trials (Liu et al., 2009). Similarly, the root mean square error of an ANN was statistically successful in predicting KJ angles and moments in the sagittal plane during gait (Mundt et al., 2019). For data sets of sequence, RNN models are the most appropriate networks due to its feedback looping mechanism and parameter sharing. By way of parameter sharing, the RNN model can efficiently predict outputs by reducing the total number of individual variables that must be learned (Graves, 2012; Goodfellow et al., 2016). This technique has been used in several studies to assess gait patterns in clinical populations (Mezghani et al., 2008; Filtjens et al., 2020) as well as to predict and classify individual pathological diagnosis (Holzreiter & Kohle, 1993; Kaczmarczyk et al., 2009; Zeng et al., 2016). Clinical gait analysis of specific events at detected times was automated by an RNN model and presented excellent outcomes of timing agreements just 10ms within manually computed outcomes (Filtjens et al., 2020).

However, one of the drawbacks of RNN models is an issue with learning over long sequences. In brief, the parameter sharing can result in an illogical explosion or vanishing of the learning gradient (i.e. sensitivity to input). Long Short Term Memory (LSTM) networks, a specific type of RNNs, were specifically designed to handle issues with gradients. Unique to LSTM, training occurs at the hidden layer via a framework of an input gate, forget gate, and output gate. During training, the LTSM cells communicate the information and distinguish the input signals into two classes (keep or forget) based on the information received and its importance. LSTMs thus provides a unique way of storing and accessing memory across cells/neurons for an extended period. As such, LSTMs have been quite successful at tasks requiring long-range memory (Chen & Chaudhari, 2004; Schmidhuber & Hochreiter, 1997; Gers & Schmidhuber, 2001). LSTM was also successfully presented by Holzreiter and Kohle (1993) when a neural network was designed to distinguish a healthy versus pathological gait pattern with GRF input data. Output values are derived by sigmoid and tangential functions and are represented as 0 (remove) and 1 (keep). Gait patterns were classified as healthy (0) and pathological (1) and so, an output value of 0.9 was predictive of a pathological gait pattern (Holzreiter & Kohle, 1993). However, it is important to note that neural network training occurs over several time sequences in a randomized fashion and is influenced by the interconnecting weights, thus not every output set will be equally successful (Luu et al., 2014). Therefore, it is pertinent to perform training in multiple iterations with different starting weights to generalize results.

Overall, neural networks are utilized to process compound data sets and problems in a way that imitates the human brains' mechanisms for information processing. Throughout this review, the non-linear relationship between kinematics and KJCF has been revealed, as well as the current complex methodologies to predict in-vivo KJ data. As such, I pose that it is possible to design a neural network, such as the very successful LSTM, to learn the relationship betweeen kinematics and KJCF using opensource in-vivo datasets, thus replacing the need for complex musculoskeletal modeling.

CLOSING STATEMENT

This review has presented the current literature on predicting in-vivo KJ data by the methods of instrumented implantations, model simulations, and kinematic and kinetic variables. However, the scarce data from instrumented implantations is consequently affected by not only the high cost of accessibility but also the infrequency of instrumented TKR procedures. Similarly, the knowledge and experience required to analyze model simulations is both complex and inefficient for those in a clinical setting. The methods presented all had the commonality of kinematics being the actual variable being measured. Therefore, it is expected that utilizing just kinematics to predict in-vivo KJCF will be the most appropriate procedure and will successfully surpass the current methods being used.

CHAPTER III
METHODS

PARTICIPANTS

This study involved secondary analyses of publicly available data. Thus, this study was exempt from institutional review board approval (IRB #: 1481294-1). The "Grand Challenge" competition to predict in-vivo knee loads and Orthoload/CAMS-Knee (K5R & K8L, retrieved from https://CAMS-Knee.orthoload.com, Taylor et al. 2017) datasets were used. Experimental data included motion capture (marker trajectory and ground reaction forces) and in-vivo instrumented knee prosthesis data (e.g., knee joint contact forces) from all datasets. Although there are six datasets in the Grand Challenge, two datasets are repeats of the same participants (JW: GC 1 and GC 4; DM: GC 2 and GC 6; Table 1). The available data was split into two groupings: training and testing. The training group included the "normal" walking conditions of all six datasets from the Grand Challenge (n=34; Table 1). The testing (to prove accuracy for similar gait conditions) group included two participants from CAMS-Knee (number of trials=5; Table 2).

Table 1. Participant demographics used for training the neural network.

	Initials	Sex	Leg	Mass	Height	Trials
GC 1	JW	M	R	64.6	166	5
GC 2	DM	M	R	67	172	5
GC 3	SC	F	L	78.4	167	5
GC 4	JW	M	R	66.7	168	5
GC 5	PS	M	L	75	180	6
GC 6	DM	M	R	70	172	8

Note: Participant data were obtained from the Grand Challenge (GC). Mass and height are reported in kilograms and centimeters, respectively. Only normal overground walking conditions were included.

Table 2. Description of participants/conditions used for validating the neural network.

	Initials	Sex	Leg	Mass	Height	Conditions (Trials)
CAMS 1	K5R	M	R	96.0	175	NORM (2)
CAMS 2	K8L	M	L	78.8	175	NORM (3)

Note: Participant data were obtained from CAMS-Knee (CAMS) and Grand Challenge (GC). Mass and height are reported in kilograms and centimeters, respectively.

KINEMATIC & KJCF DATA PROCESSING

Raw motion capture and GRF data from both the Grand Challenge and CAMS-Knee datasets were low pass filtered using a second order, zero-lag butterworth filter with a cutoff frequency of 6 Hz. Musculoskeletal modeling was performed using OpenSim (v3.3, SimTK, Stanford, CA) and the Lai 2017 model. The standard torso and lower extremity model (3 dof for torso, 6 dof for the pelvis, 3 dof from the hip, 1 dof for the knee (flexion/extension), and 1 dof for the ankle) was modified to include frontal plane motion of the knee joint (Bennett et al., 2020). This modified model has been previously validated using data from the sixth Grand Challenge (Bennett et al., 2020). The standard model was then scaled to each participant's height, mass, and segment lengths. Next, inverse kinematics-based joint angles and pelvis positions were solved for at each frame using a least-squares approach while accounting for constraint weights (Spoor & Veldpaus, 1980). Kinematic and KJCF data were filtered at 6Hz. The KJCF data (provided in the Grand Challenge and CAMS-Knee datasets) were then used to calculate medial and lateral compartment joint contact forces using previously defined equations and normalized to body weight (Zhao et al., 2007). Kinematic and KJCF data were time-normalized to the stance phase, defined using 10N thresholds of the vertical GRF, and then imported into MATLAB (R2016B, The Mathworks, Inc., Natick, MA). Ensemble kinematic data for the CAMS datasets against the training dataset are provided in Figure 1. Ensemble medial and lateral knee joint contact forces for the training and testing datasets are provided in Figure 2.

Figure 1. Ensemble kinematic data for the CAMS datasets with the training data.

Figure 1 Caption: Sagittal plane (first column), frontal plane (second column), and transverse plane (last column) kinematic data are provided for the hip (first row all columns), knee (second row all columns), ankle (third row first column), trunk (third row second column). The solid black line and shading are the mean and one standard deviation of the training dataset. CAMS 1 and CAMS 2 kinematics are the dashed and dash-dot lines, respectively.

Figure 1. Ensemble kinematic data for the CAMS normal gait against the GC normal gait (training dataset).

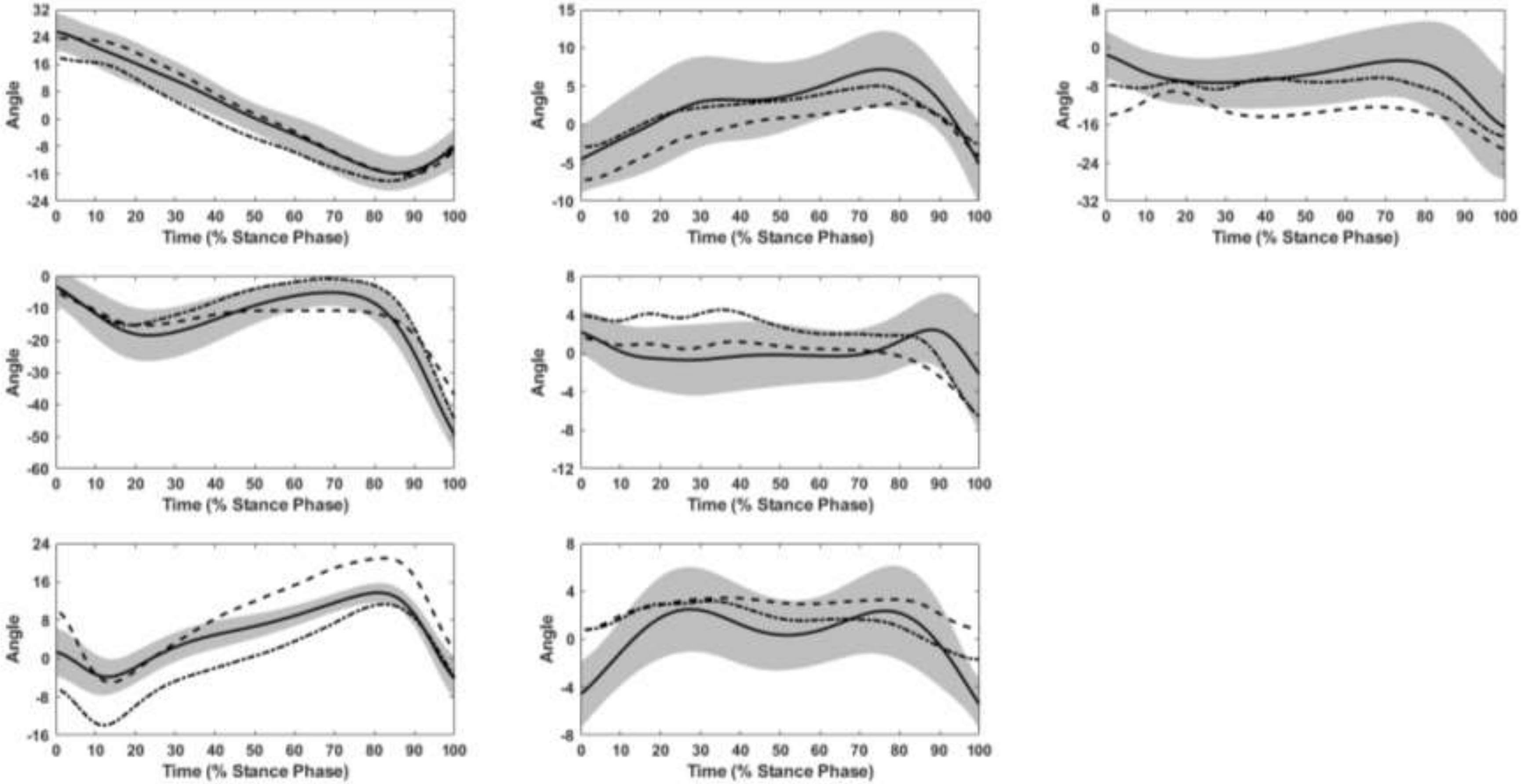

Figure 2. Ensemble medial and lateral knee joint contact forces for the training and testing datasets.

Figure 2 Caption. Mean (solid lines) and one standard deviation (shaded region) medial and lateral knee joint contact forces are presented for the training dataset. Mean forces for CAMS 1 and CAMS 2 are the dashed and dot-dash lines, respectively. Forces are normalized to body weight (BW).

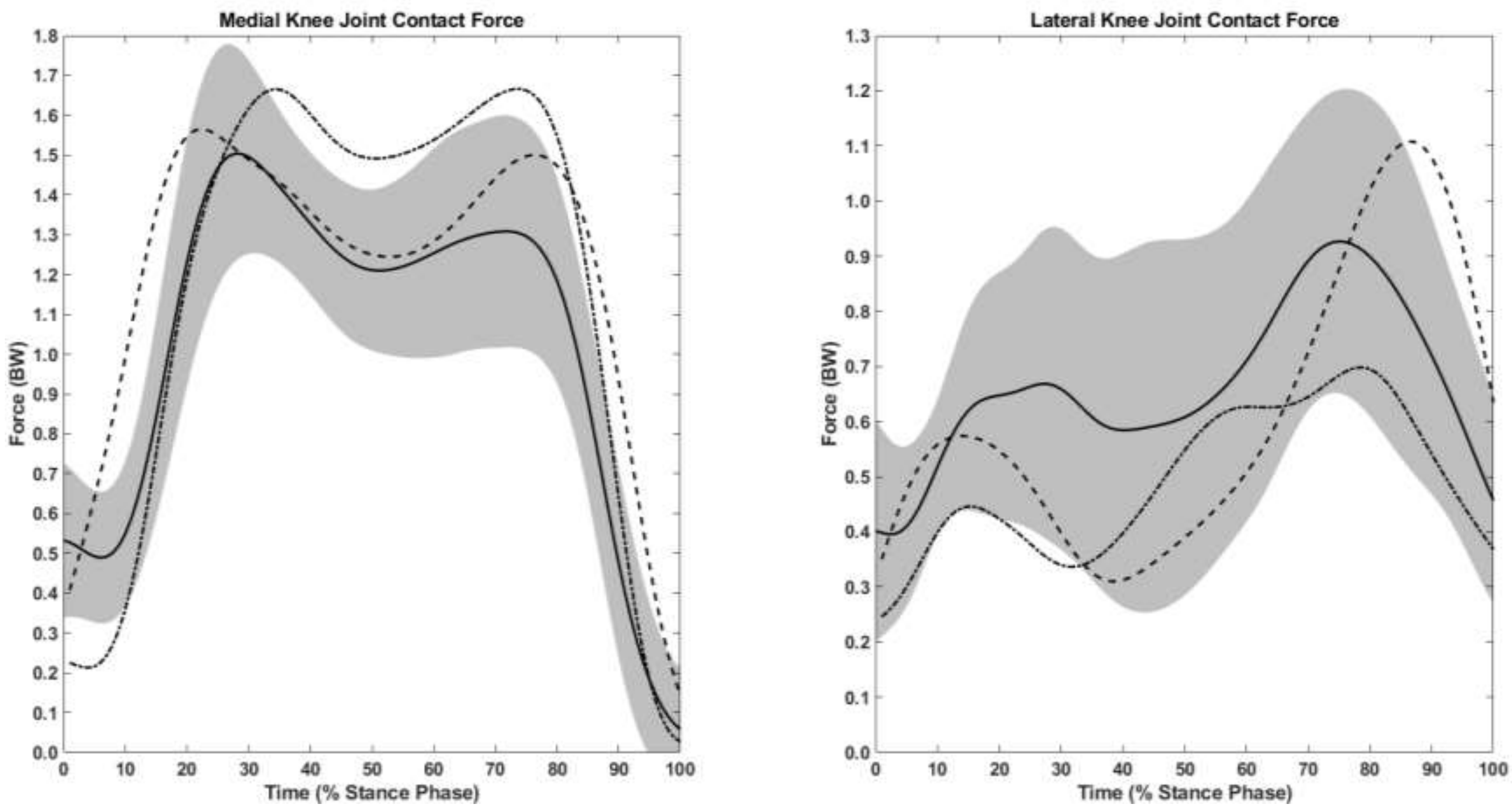

MODEL DESIGN OF NEURAL NETWORK

Using MATLAB neural network tools, a 3-layer (input layer, hidden layer, and output layer) recurrent neural network, specifically the long-short term model, was designed to predict KJCF from selected kinematic elements. The kinematic inputs were as follows: hip (frontal, sagittal, transverse), knee (sagittal and frontal), ankle (sagittal), and trunk (frontal), determined as significant factors related to KAM and KJCF by previous literature (Mündermann et al., 2008; Sasaki et al., 2010; Teng et al., 2014; Richards et al., 2018). We assumed knee kinematics must be included for the network to be anatomically relevant. Therefore, only combinations of the 7 kinematic elements that include at least one knee kinematic element were used, resulting in 96 different input models.

There are several factors of an RNN that should be considered when designing a network: initial weights and biases, hidden layer size, mini batch size, and training optimization algorithm, along with regularization to combat overfitting. The weights and biases (4 each: input, forget, and output gates and cell candidate) of the input and recurrent layers are "updated" each training iteration (epoch) to improve model fit on the training data. Initial settings for layer weights (initial and recurrent) can be produced via random number generators: Glorot, He, and Narrow-Normal (sampling from a narrowed normal distribution) (Glorot & Bengio, 2010; He et al., 2015). A subset of the full training dataset (normal for training data) was used to compare the weight initializers by comparing convergence of validation (i.e. plotting accuracy over epochs). The initializer that converges fastest with the best validation will be chosen for implementation in the training of the full dataset. In addition to the initializer, the random nature of the initial weights should be considered. Therefore, each of the 1,824 input models was also be trained 5 times using different random numbers (total 9,120 models).

The number of hidden units of the hidden layer (singular layer in an LSTM) represents the number of neurons involved (or the amount of information remembered between time steps). Currently, there is no “best set” for the appropriate size/number of neurons in an LSTM. As such, the appropriate size was determined by creating each of the 96 input models with 2-20 neurons (total 1,824 models). Mini-batch size represents the amount of data, trials in the current case, that are fed from the input to the hidden layer at each epoch. Sizes can range from 1 to the full dataset. Although fitting each individual trial would be optimal for training, this can hinder generalizability. Minibatches (size=3, n=11) were also be randomized per epoch to enhance generalizability.

Network training in MATLAB can be performed by a few variants of stochastic gradient descent: Stochastic Gradient Descent with Momentum (sgdm), Root Mean Square Propagation (RMSProp), and Adaptive Moment Estimation (Adam). As current literature is not in agreement on the best optimizer, comparisons of each optimizer were performed in a similar methodology to the layer weight initializers (Wilson et al., 2017). Weight regularization involves imposing constraints on the input and/or recurrent weights of the LSTM, with the goal of reducing overfitting and improving performance (Bishop, 2006; Murphy, 2012). The standard regularization method in MATLAB is L2Regularization with a default weight decay of 0.0001.

NETWORK SELECTION

Multiple methods, both quantitative and qualitative, exist to determine the relationship between two waveforms. Here, we examined strength of relationship between networks and in-vivo data through continuous (waveform agreement) and discrete (agreement of 1st and 2nd peaks) aspects based on the current literature.

First, the proportion of the variance explained (correlation coefficient squared (R^2)) and the root mean square error (RMSE) between in-vivo test data and network predictions (mean of all 5 iterations per network for generalizability) represent determine network waveform accuracy. Assumedly, many networks could achieve similar levels of accuracy, even from the same kinematic combinations (e.g., knee flexion-20 neurons and knee flexion 10 neurons). Therefore, to reduce the number of networks to compare, we implemented minimum thresholds (RMSE≤0.50 and R^2≥0.49) determined by results reported in the literature (Zhao et al., 2007; Jung et al., 2017; Chen et al., 2014; Lerner et al., 2015; Mundt et al., 2020; Oh et al., 2013). The minimum thresholds yielded over 800 networks, suggesting more stringent criteria were necessary. Therefore, the thresholds were incrementally increased (RMSE = 0.50:0.05:0.00 and r=0.70:0.05:1.00) until only networks representing 5 different kinematic combinations or fewer fulfilled the criteria (Table 3). Fifteen networks (3 different kinematic combinations) achieved R^2≥0.64 and RMSE≤0.30. Twenty-three networks (repeat of 1 kinematic combination from R^2≥0.64 and RMSE≤0.30; 2 new kinematic combinations) successfully met RMSE≤0.40 and R^2≥0.7225 (i.e., r≥0.85). These five networks were compared further, as their performance was exceptional (Table 3).

Table 3. Number of networks that met set thresholds

r, R^2	*RMSE*	*n* models	Kinematic combinations
0.70, 0.49	0.30	15	3
	0.35	187	41
	0.40	732	63
	0.45	874	67
	0.50	877	67
0.75, 0.56	0.30	15	3
	0.35	173	41
	0.40	456	58
	0.45	476	58
	0.50	476	58
0.80, 0.64	0.30	15	3
	0.35	78	24
	0.40	123	27
	0.45	123	27
	0.50	123	27
0.85, 0.72	0.30	12	1
	0.35	21	2
	0.40	23	3
	0.45	23	3
	0.50	23	3
0.90, 0.81	0.30	11	1
	0.35	11	1
	0.40	11	1
	0.45	11	1
	0.50	11	1

Although a network can achieve strong predictor values of a high correlation with a low RMSE, it is important to note that this does not necessarily assure that the predicted waveform corresponds with the “m-shaped” waveform assumed by in-vivo data during normal gait. Correlations coefficients can be greatly influenced by the longer loading and pushoff phases of the gait cycle, allowing the midstance “valley” to be less represented. Therefore, an additional parameter to determine the best LSTM network was to visually examine (i.e., the qualitative waveform assessment) the predicted output by each of the five iterations for the best performing network groups for the expected “m-shape”. The representative network for each of the five kinematic combinations was chosen as the trial that presented with the waveform fit to the in-vivo data.

In addition to waveform assessments, analyzing discretized data is an important factor for KJCF. The 1st (i.e., loading response peak, 0-50% stance) and 2nd (i.e., pushoff peak, 50-100% stance) peak forces and their respective timings for each of the five representative networks was calculated. The forces (BW) and their timings were compared to the 1st and 2nd peak forces and timings obtained from the testing dataset.

The performance of the best network for each of the kinematic combinations are provided and compared in the Results section. Finally, the contributions of each kinematic element to the accuracy of the overall best network (see Results section) was analyzed by systematically removing each variable from the network (akin to Type III Sum of Squares). Performance is then reported for each new network via RMSE and R^2.

CHAPTER IV
RESULTS

THE BEST REPRESENTATIVE NETWORKS

Table 4 describes the five best networks and their performance in predicting the testing (CAMS) dataset. Figure 3 presents the mean network predictions compared to in-vivo data for each of the CAMS subjects. Figure 4 presents the differences in peak forces and the timing of peak forces between each network and the in-vivo data. Network predictions for each trial per CAMS subject can be found in the Appendix.

Table 4. Fit of the five best networks on the CAMS datasets.

			Medial		*Lateral*	
Network	**Neurons**	**Kinematic Inputs**	***RMSE***	***R^2***	***RMSE***	***R^2***
1	15	Kn Flx/Ext	0.24	0.84	0.26	0.06
2	20	Kn Flx/Ext, Hip Flx/Ext, Ank Dr/Pl	0.33	0.77	0.32	0.02
3	8	Kn Ad/Abd, Hip Flx/Ext, Hip Ad/Abd, Ank Dr/Pl	0.27	0.77	0.18	0.08
4	20	Kn Flx/Ext, Hip Flx/Ext, Hip Int/Ext, Ank Dr/Pl	0.31	0.77	0.38	0.05
5	18	Kn Flx/Ext, Kn Ad/Abd, Hip Int/Ext, Ank Dr/Pl	0.24	0.80	0.24	0.07

Notes. Kn and Ank: knee and ankle, respectively. Flx/Ext: Flexion and extension, Ad/Abd: adduction and abduction, Int/Ext: internal and external rotation, Dr/Pl: dorsiflexion and plantarflexion motions, respectively.

All five networks demonstrated excellent fit with the training data, achieving RMSE < 0.26BW for medial and lateral forces, $R^2 > 0.69$ for medial forces, but only $R^2 > 0.15$ for lateral forces. For the test dataset, the network with only sagittal knee kinematics (Network 1) provided the greatest R^2 (0.84) and tied for the lowest RMSE (0.24). Similarly, Network 5, consisting of four kinematic elements, produced strong accuracy with the CAMs dataset. However, as can be found in Figure 3, both Network 1 and Network 5 produced poor “m-shape” waveforms for CAMS 1. Network 1’s peak force and timings were among the worst of the networks (Figure 4). The most consistent (across all CAMS datasets) predictions of the “m-shape” are Network 2 and Network 4, which also had the highest RMSE. Fit for the lateral forces was poor across all networks (Table 4). Networks 3 and 5 produced the most accurate medial and lateral peak forces and timings of peak forces.

For subject CAMS1, network 3 starkly yielded the best output predictions for all trials in comparison to network 5. On the other hand, the differences in CAMS2 output predictions per trial by networks 3 and 5 were not as conspicuous. Consequently, through the process of elimination concerning predictions for each of CAMS2 corresponding trials, network 3 generated slightly more consistent waveform patterns that resemble the desired "m-shape" than network 5. In line with this and the starkly stronger performance for CAMS1, network 3 was confirmed to be the overall best LSTM model for medial KJCF predictions.

The effects of each kinematic element to the success of Network 3 are provided in Table 5. Sagittal ankle and frontal hip kinematics appear to have the greatest effects, as removal of these dramatically increased error (RMSE) and decreased waveform agreement (R^2). Frontal knee kinematics had the least effect on waveform agreement (R^2); however, removal of any variable resulted in at least a 30% increase in RMSE.

Table 5. Accuracy statistics of each reduced network.

	KINEMATIC COMBINATION	MEDIAL KJCF		LATERAL KJCF	
		RMSE	R^2	RMSE	R^2
Reduced Network	A-DP Removed	0.45	0.40	0.15	0.50
	H-Ad Removed	0.37	0.52	0.20	0.11
	H-FE Removed	0.36	0.63	0.19	0.07
	K-Ad Removed	0.35	0.72	0.20	0.26
Full	K-AD, H-FE, H-AD, A-DP	0.27	0.77	0.18	0.08

Notes. Ad: adduction/abduction motion; FE: flexion/extension motion; DP: dorsiflexion/plantarflexion motion; A, K, H: ankle, knee, and hip, respectively. RMSE: root mean square error in body weight. R^2: correlation coefficient squared.

Figure 3. Ensemble network predictions of CAMS datasets.

Figure 3 Caption. In-vivo data (mean: solid black lines, standard deviation: shaded regions) for CAMS 1 (A) and CAMS 2 (B) are provided. Mean predicted forces by networks 1-5 are the dashed black, dash-dot black, solid gray, dashed gray, and dotted grey lines, respectively.

Figure 3A. Ensemble network predictions of CAMS 1.

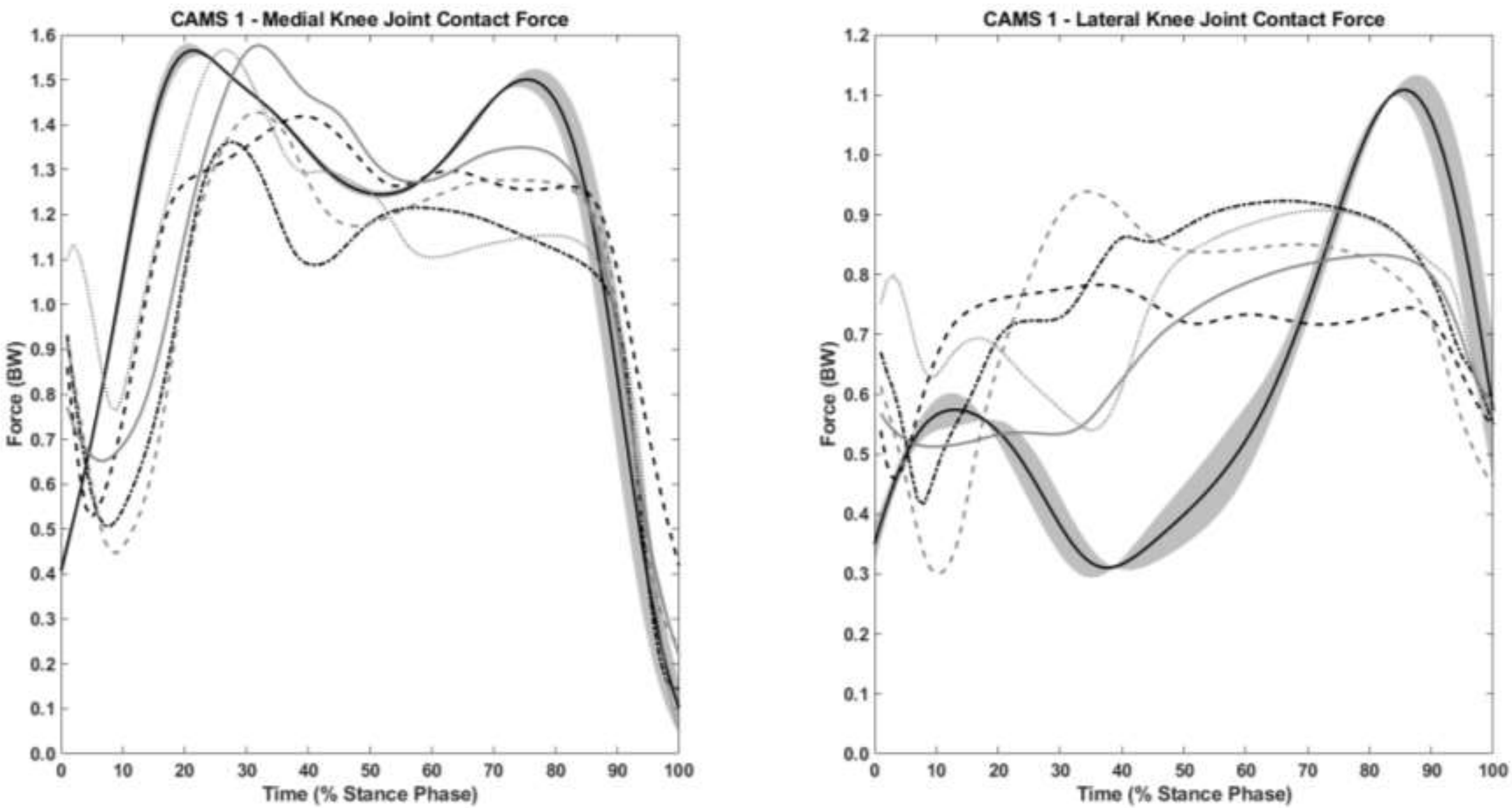

Figure 3B. Ensemble network predictions of CAMS 2.

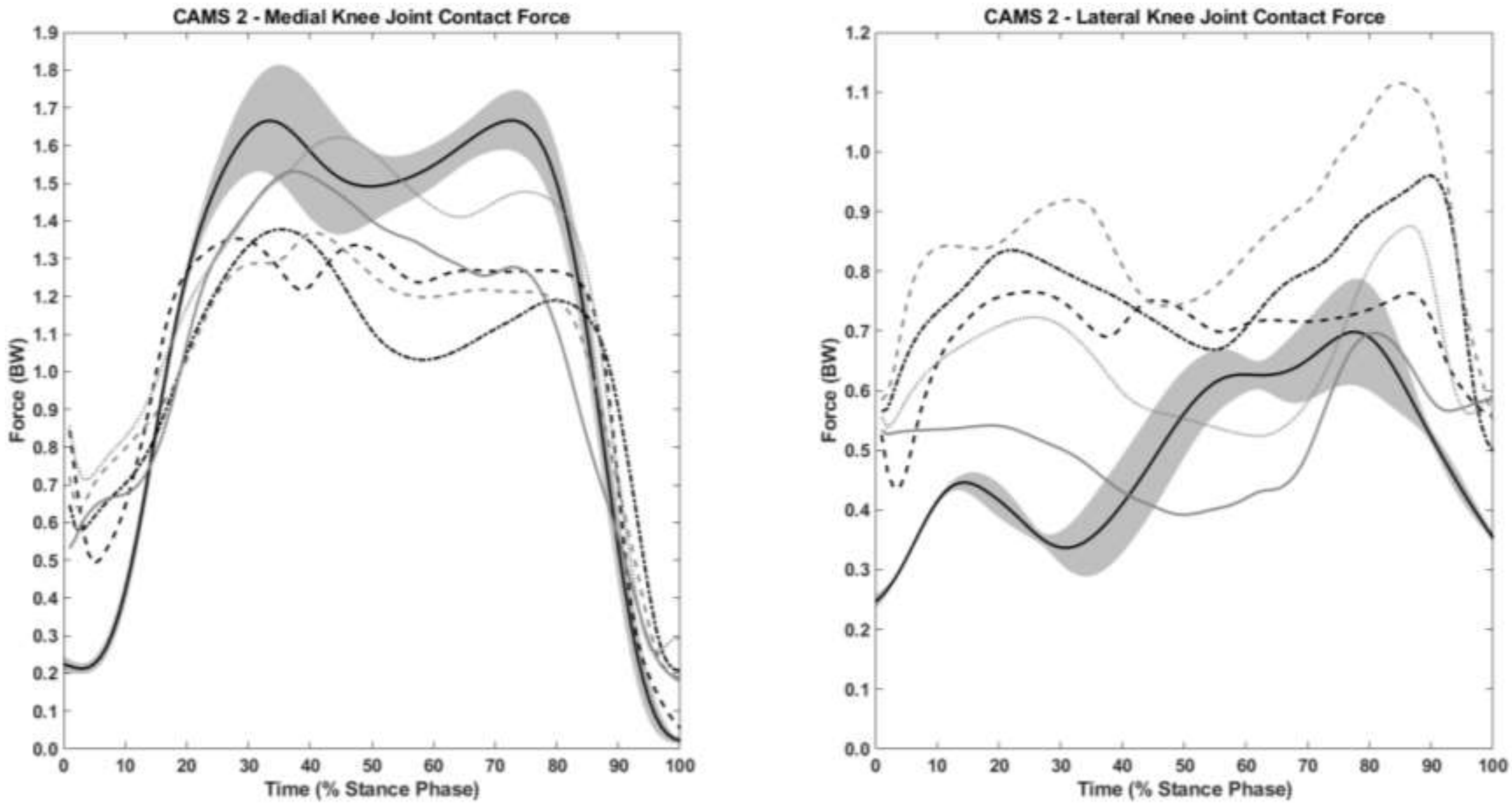

Figure 4. Differences between network predictions and in-vivo waveform peak forces and timing of peak forces.

Figure 4 Caption. Average (CAMS 1 & 2) differences in peak forces (A) and timing of peak forces (B) are provide for networks 1-5: solid black, dark gray, light gray, dotted, and diagonal stripes, respectively. Errors for medial (MED) and lateral (LAT) first (1; within first half of stance) and second (2; within second half of stance) peaks are presented.

Figure 4A. Differences in peak forces between networks and in-vivo data.

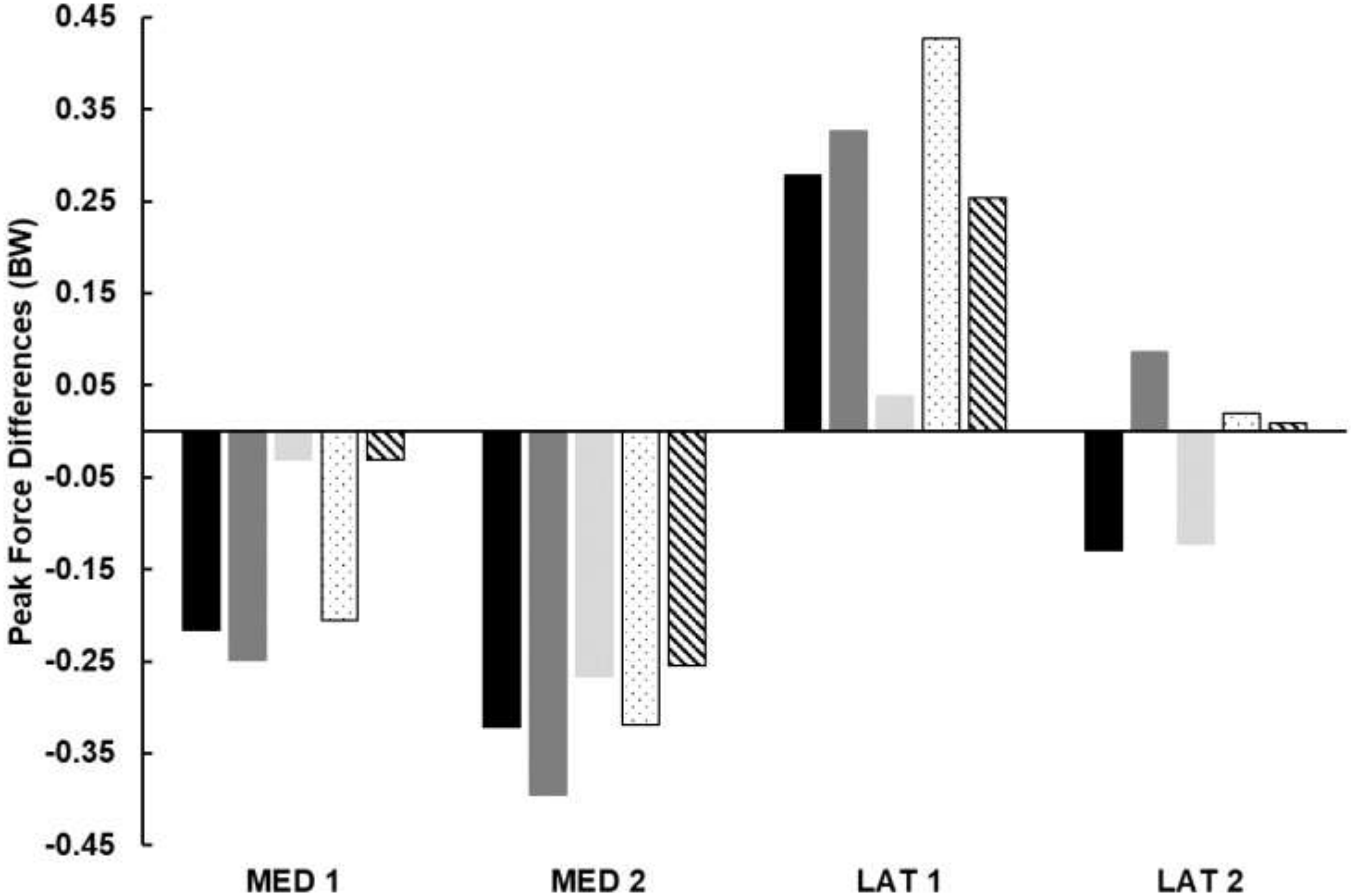

Figure 4B. Differences in timing of peak forces between networks and in-vivo data.

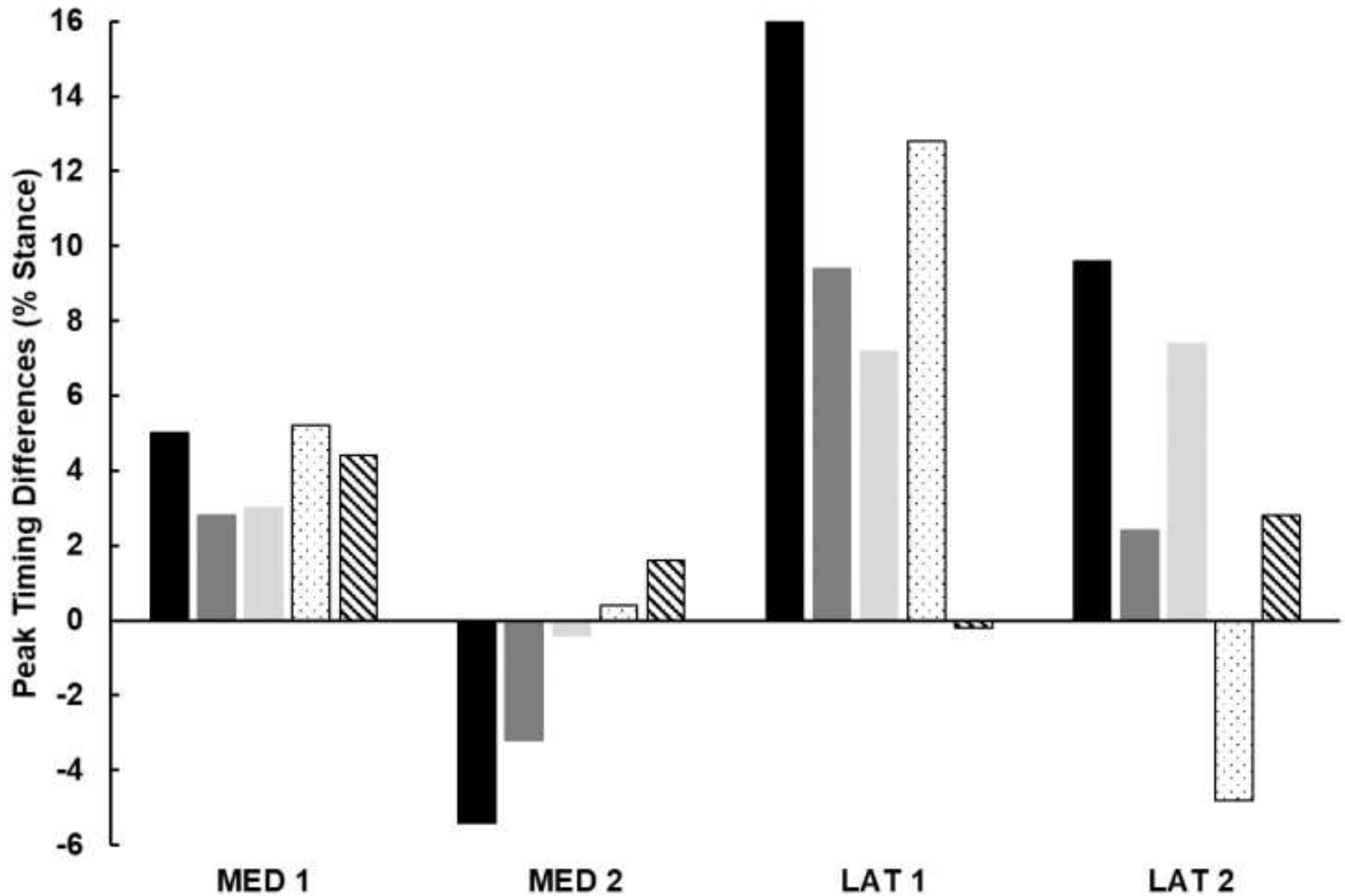

CHAPTER V
DISCUSSION

The aim of this study was to develop a methodology for predicting bone on bone forces at the knee that is comparable to the traditional methods of musculoksletal modeling and surrogate measures via external KAMs, but requiring less expertise and equipment. We proposed that an LSTM network composed of only kinematic inputs would predict KJCF with greater levels of accuracy than those reported using musculoskeletal modeling. Further, we also hypothesized that more than one combination of kinematic variables would match the level of accuracy reported by musculoskeletal modeling techniques.

NETWORK PREDICTIONS VS MUSCULOSKELETAL MODELING AND KAMS

When discussing our results with those from previous studies, it is important to note that the medial compartment is typically the focal point throughout the current literature, as predictions of lateral compartment forces are generally much worse and of lesser interest. Though we are not aware of analyses associating joint kinematics specifically with lateral knee joint loading, predictions of lateral compartment forces by musculoskeletal modeling are very variable (Smith et al., 2016; Jung et al., 2016; Marra et al., 2015; Knarr & Higginson 2015; Ding et al., 2016; Lundberg et al., 2013). Possible attributes of this limitation can be due to individual static and dynamic profiles of joint alignment (Hurwitz et al., 2002; Noble et al., 2006; Mündermann et al., 2008; Kia et al., 2014). Additionally, subject-specific kinematic and kinetic responses can occur with TKRs (Bade et al., 2010; Komnik et al., 2016; Mundt et al., 2020). Considering this, it is interesting to note that although our reported waveform agreement (R^2) for lateral compartment forces were poor, our waveform error (RMSE) and peak data (magnitude and timing of peaks) revealed good agreement with the in-vivo data. From this standpoint, it can be further presumed that joint kinematics demonstrate a prominent role in both compartments of the knee joint. It is entirely possible networks optimized to medial and lateral compartment loading separately would contain different kinematic combinations. Future research should examine the mechanisms behind lateral compartment loading

Overall, the five representative LSTM networks achieved an accuracy level greater than those reported by musculoskeletal modeling during normal gait (Smith et al., 2016; Marra et al., 2015; Ding et al., 2016). It is apparent that all five LSTM networks outperform most musculoskeletal models with reported correlations of 0.55-0.81 (RMSE=0.22-0.56BW) (Jung et al., 2016; Jung et al; 2017; Smith et al., 2016; Ding et al., 2016) with the exception of a few single-subject studies that have slightly higher correlations (0.79-0.96) (Marra et al., 2015; Manal and Buchanan 2013; Chen et al., 2014). The greater prediction accuracies in those studies were attained by incorporating additional subject-specific parameters of electromyography (Manal and Buchanan 2013) and knee alignment (Marra et al., 2015). Inclusion of individualized parameters for subject-specific model design can improve KJCF predictions (Kia et al., 2014; Ding et al., 2016; Manal & Buchanan 2013); however, this approach limits generalizability (Knarr and Higginson 2015; Lerner et al., 2015; Kia et al., 2014) and requires additional testing/equipment and training. Additionally, the requirement of inverse dynamic, muscle excitation, and joint contact force computations for musculoskeletal model design must be recognized as a limitation in that it is not only time-consuming for repeated subjects but also requires extensive background knowledge. Thus, our LSTM network should be considered a highly accurate alternative method to musculoskeletal modeling for predicting KJCF. In addition, we believe our LSTM network provides an improved generalizable approach for ascertaining in-vivo data for researchers and clinicians alike – not just those without the requisite knowledge and capability to implement subject-specific musculoskeletal modeling.

LSTM VS KAMS

Equally important is to note our networks' prediction results with KAMs, a surrogate measure of KJCF (Kutzner et al., 2010; Zhao et al., 2006; Walter et al., 2010; Mundermann et al., 2018). Research typically implements KAM in the form of discrete data with the assumption that greater peak KAMs indicate greater peak medial compartment contact forces during gait (Sparkes et al., 2019; Bennell et al., 2011; Nie et al., 2019; Messier et al., 2005; Meireles et al., 2016). During normal gait trials, average correlation coefficients squared (R^2) between 1st and 2nd peak KAMs and medial compartment forces range from 0.29-0.69 and 0.20-0.60, respectively (Walter et al., 2010; Kutzner et al., 2010; Meireles et al., 2016). Though, it must be mentioned a similar average correlation of medial KJCF with KAM for one subject throughout stance was reported by Zhao et al. and is in agreement with our networks 2-4 (R^2=0.77) (2006). In contrast to KAMs, the LSTM network presented here allows for the direct prediction of medial contact forces for the entirety of a full gait cycle and discrete 1st and 2nd peaks that are common of research interest (Zhao et al., 2007; Walter et al., 2010; Kutzner et al., 2010; Meireles et al., 2016), yet requires less information than KAMs. Furthermore, despite the utility of KAMs as a surrogate measure of medial compartment forces, the strong relationship between KAMs and medial contact forces may not be robust to gaits other than "normal" (Walter et al., 2010).

Support for the success of the LSTM networks built only from kinematic data can be gleaned from the derivation of KAMs (Kutzner et al., 2013; Meireles et al., 2016; Richards et al., 2018). The KAM is essentially a product of ground reaction force (GRF) and its lever arm (assuming foot mass is negligible). As such, previous research has found magnitudes of KAM are more associated (R^2=0.77) with the change in frontal plane tibiofemoral alignment (i.e., knee kinematics) than GRF (Hunt et al., 2006). This finding is greatly supported by our results demonstrating the crucial impact that kinematics have on compartmental forces at the knee joint. Even further, our results exemplify the proposed method is an accurate approach for predicting KJCF by utilizing only kinematic parameters rather than obtaining GRF data and solving for three-dimensional knee joint moments to present as surrogate measures. Additional advantages include the practicality and generalizability for predicting accurate medial KJCF in almost all general populations and the opportunity to also measure knee joint impulse (which requires data for the KJCF waveform).

NETWORK KINEMATIC VARIABLES AND COMBINATIONS

During gait, it is evident that joint kinetics and kinematics constitute a complex relationship. Changes in kinematics at one joint affect the kinematics at the subsequent joints and consequently impacts the force/moment output. Considering this, the innate individual characteristics of lower-extremity joint alignment during gait can be attributing factors to help us understand discrepancies in the networks' waveform predictions.

As discussed, previous literature has not evaluated the complex relationship between kinematics and joint contact forces, let alone predicted KJCF using only kinematic parameters. Our proposed recurrent neural network with an LSTM design not only confirmed that is possible but also revealed that there is a strong (high accuracy) and physiologically relevant association between lower extremity kinematics and knee joint contact forces. Given this study included a majority of the available degrees of freedom within the lower extremity, it can be assumed that nearly all of the possible kinematic combinations (which were required to include at least one knee kinematic element) could be trained to be moderately/strongly accurate prediction networks. However, the higher-level performance on the test dataset should be exemplified by kinematic elements that are reliably related to KJCF (as training was performed using four different participants kinematics/KJCF) and are founded on biomechanical principles. In this vein, kinetics (i.e. KJCF) during the loading and propulsion phases of gait are influenced by several kinematic parameters (Van Den Noort et al., 2013; Shull et al., 2013; Richards et al., 2018; Bennett et al., 2020; Simic et al., 2013, Shull et al., 2013; Hunt et al., 2006). In agreement with the previous literature, the representative networks contain relevant kinematic combinations that reportedly influence KJCF (Shull et al., 2013; Richards et al., 2018; Bennett et al., 2020). The emergence of each representative network, in comparison to their lower-performing counterparts, is a function of the apparent differences in kinematics between the testing and training datasets (see Figure 1). For instance, sagittal plane ankle, hip internal/external rotation, and knee adduction/abduction kinematics for the CAMs subjects vary beyond the expected waveforms of the GC subjects, even though this is only normal gait.

The highest R^2 attained was by Network 1, which included only sagittal knee kinematics as the input variable. In fact, eleven networks (different # neurons) including only sagittal plane knee kinematics achieved R^2 >0.81 and RMSE <0.30 BW, clearly establishing it as the strongest predictor of KJCF. In contrast, the best-selected LSTM model was network 3 and did not include the sagittal knee variable. We observed a more accurate waveform representation of KJCF predictions, driven by the network's design that included two frontal plane variables (hip/knee) and two sagittal plane variables (hip/ankle). Each of these variables has been previously identified as physiologically relevant to the knee joint loading during walking. For instance, static and dynamic frontal plane tibiofemoral alignment are strongly related to medial KJCF during gait (Simic et al., 2013, Shull et al., 2013; Bennett et al., 2017; Bennett et al., 2020; Van

Den Noort et al., 2013). In addition, the location of the center of mass/pelvis in the frontal plane can draw the GRF further/closer to the mechanical axis of the knee joint and affecting the knee joint load (Hunt et al., 2006; Walter et al., 2010; Mundermann et al., 2018; Bennett et al., 2017; Shull et al., 2013; Guo et al., 2007).

Of particular interest is the crucial influence of sagittal ankle kinematics (see Figure 1 containing kinematic data for testing data compared to the training dataset). Focusing on our chosen best network (Network 3), it can be seen that the sagittal ankle parameter presents the greatest impact on the network's total output prediction (Table 5). During gait, adequate dorsiflexion assists with lower limb midstance, whereas successive propulsion is greatly aided by plantarflexion. If there are insufficiencies in ankle dorsiflexion range of motion, the knee joint consequently suffers (i.e. buckling of the knee). Demonstrated in clinical gait retraining studies, plantarflexor strength training has been proposed to help improve sagittal knee range of motion; therefore, assisting in re-normalization of gait (Knarr et al., 2013; Frisk et al., 2019). This implication exhibits the influential effects of each joint functioning about the lower extremity kinetic chain during gait. Considering the biomechanical function of the proximal and distal joints/segments about the knee, it can be implied that implementation of the sagittal hip and ankle successfully compensates for the exclusion of the sagittal knee parameter in network 3's kinematic combination, illustrating the effects of the kinetic chain.

Likewise, others have shown gait modifications at the foot about the transverse plane have meaningful consequents at the hip, ankle, and knee joints within the frontal plane, along with the innate simultaneous joint alterations by any individual gait modification (Simic et al., 2013, Shull et al., 2013; Bennett et al., 2017; Bennett et al., 2020; Van Den Noort et al., 2013). For example, walking with modified toe-in or toe-out angles naturally corresponds with internal/external rotation of the hip (Simic et al., 2013; Bennett et al., 2017). Therefore, we felt it is justified to include just the hip as the transverse variable, instead of including knee (truly dependent) and/or ankle transverse kinematics. In agreement with the previous literature, hip internal/external rotation emerged as an important factor of three of the representative networks.

Lastly, though trunk sway did not appear in any of the kinematic combinations for the top five LSTM networks, several studies have analyzed the association between frontal plane trunk sway and medial KJCF loading (Van Den Noort et al., 2013; Mündermann et al., 2008; Shull et al., 2013). The major target of increased trunk sway is to shift the frontal plane GRF to reduce medial compartment loading. Therefore, trunk sway was considered an important variable to include as an input (Mundermann et al., 2018; Kinney et al., 2012; Hálfdanardóttir et al., 2020; Walter et al., 2010; Van Den Noort et al., 2013). As this study included normal gait, this null finding is not an alarming result. It is certainly possible that inclusion of trials with gait modifications like purposeful trunk sway or medial thrust patterns could result in trunk sway emerging as an important variable in the network.

FUTURE DIRECTIONS

Given the success of the LSTM network output predictions, future studies should aim to replicate the results with larger samples of in-vivo data. Implementation of a larger dataset can be easily built into the LSTM and will help further establish the robustness of the network's generalizability and possibly improve the network's prediction accuracy. Furthermore, additional designs of machine learning networks for sequential data predictions may be considered. This study presented predictions of concurrent compartmental medial and lateral KJCF. However, further investigation is warranted for improving medial and lateral KJCF predictions by the design of an LSTM network with independent outputs. More information on this may help to establish a greater understanding of what the most influential lower-extremity kinematic parameters are during normal gait.

CONCLUSION

In summary, this study has shown our LSTM network can successfully predict KJCF using only input parameters of kinematic variables. Overall, our results outperformed predictions of medial KJCF by those of complex musculoskeletal modeling. In contrast, the networks' lateral predictions were not good; however, comparatively, this is of similarity in that musculoskeletal modeling predictions of the lateral knee compartment are inferior to those for the medial knee compartment (Zhao et al., 2007; Marra et al., 2015; Ding et al., 2016). Given that data of the medial knee compartment is of greater biomechanics interest and more relevant to clinical populations, our LSTM network can still be concluded to be the more practical method for its generalizability and exclusion of the complex skills that are requisite for musculoskeletal modeling. It can also be concluded that our network presents itself to be a superior method to predict medial KJCF compared to surrogate measures of KAMs (Zhao et al., 2007; Walter et al., 2010; Kutzner et al., 2010; Meireles et al., 2016).

The design of our network with an LSTM allows for generalizability and real-life applications of complex time series data and illustrates the non-linear relationship of kinematics and KJCF. Thus, it is seemingly kinematics that drives joint kinetics. These results provide a prospective mechanism for predicting bone on bone forces requiring less equipment, time, and expertise. Thus, this methodology is advantageous for future work by researchers and clinicians alike.

APPENDICES

Figure 4. Flowchart of the process behind narrowing the total networks analyzed

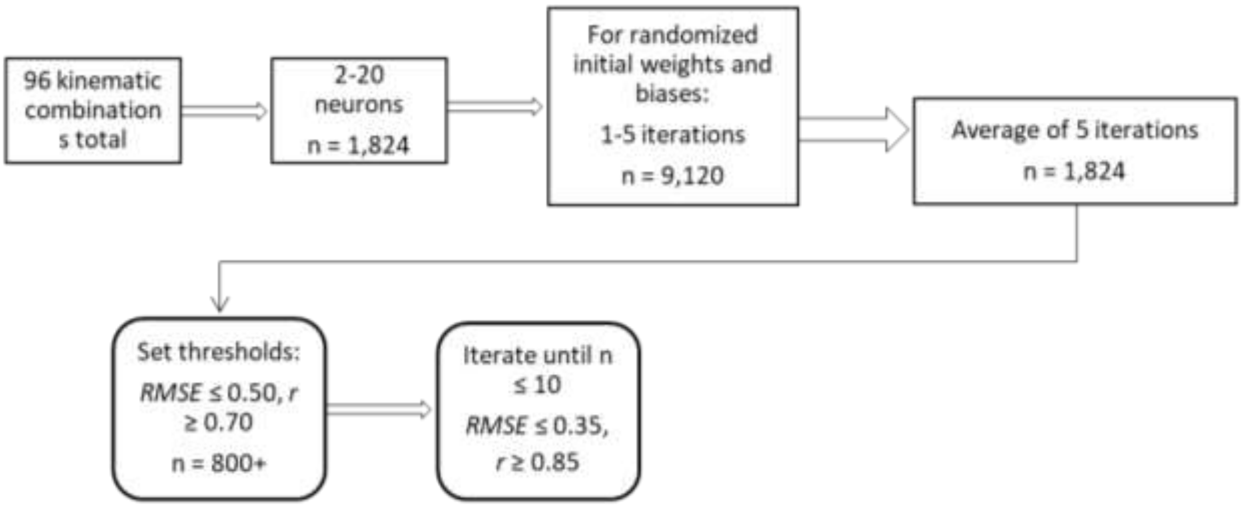

Appendix Figure 5. Network 1 predictions per trial for each CAMS subject.

Appendix Figure 5 Caption. In-vivo and Network 1 predictions of knee joint contact forces are the solid and dashed lines, respectively.

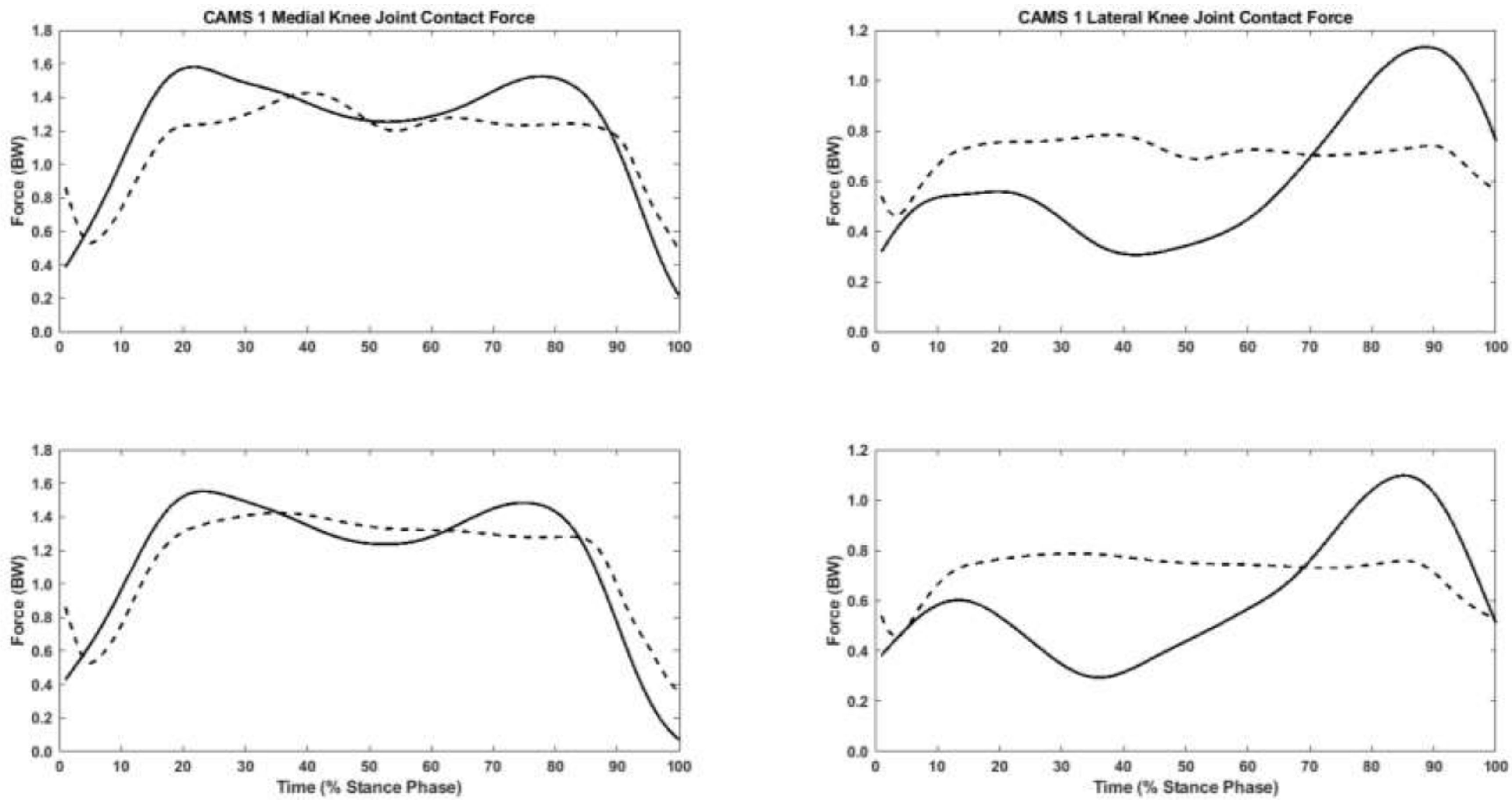

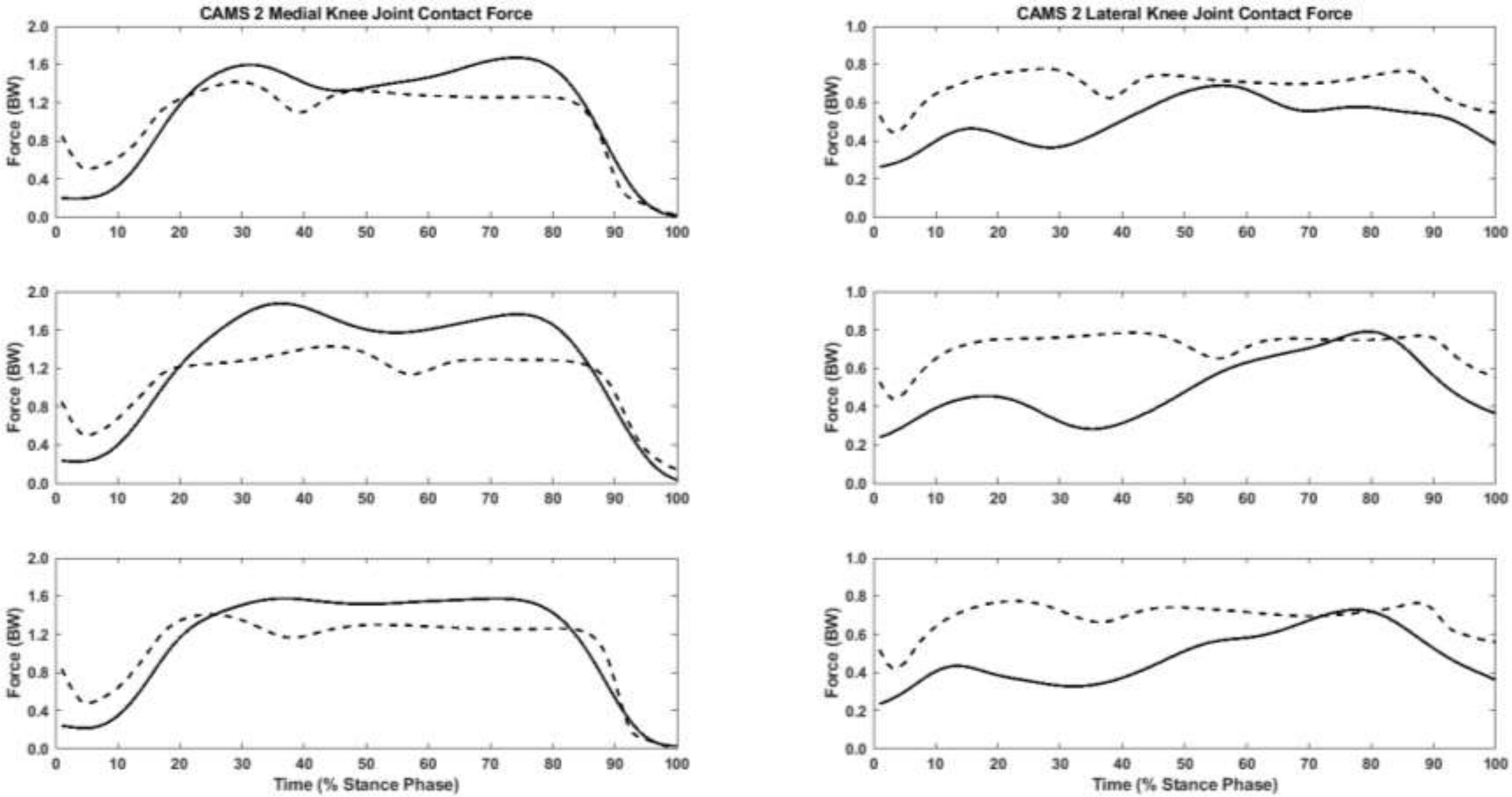
CAMS 2 Medial Knee Joint Contact Force
CAMS 2 Lateral Knee Joint Contact Force
Force (BW)
Time (% Stance Phase)

Appendix Figure 6. Network 2 predictions per trial for each CAMS subject.

Appendix Figure 6 Caption. In-vivo and Network 2 predictions of knee joint contact forces are the solid and dashed lines, respectively.

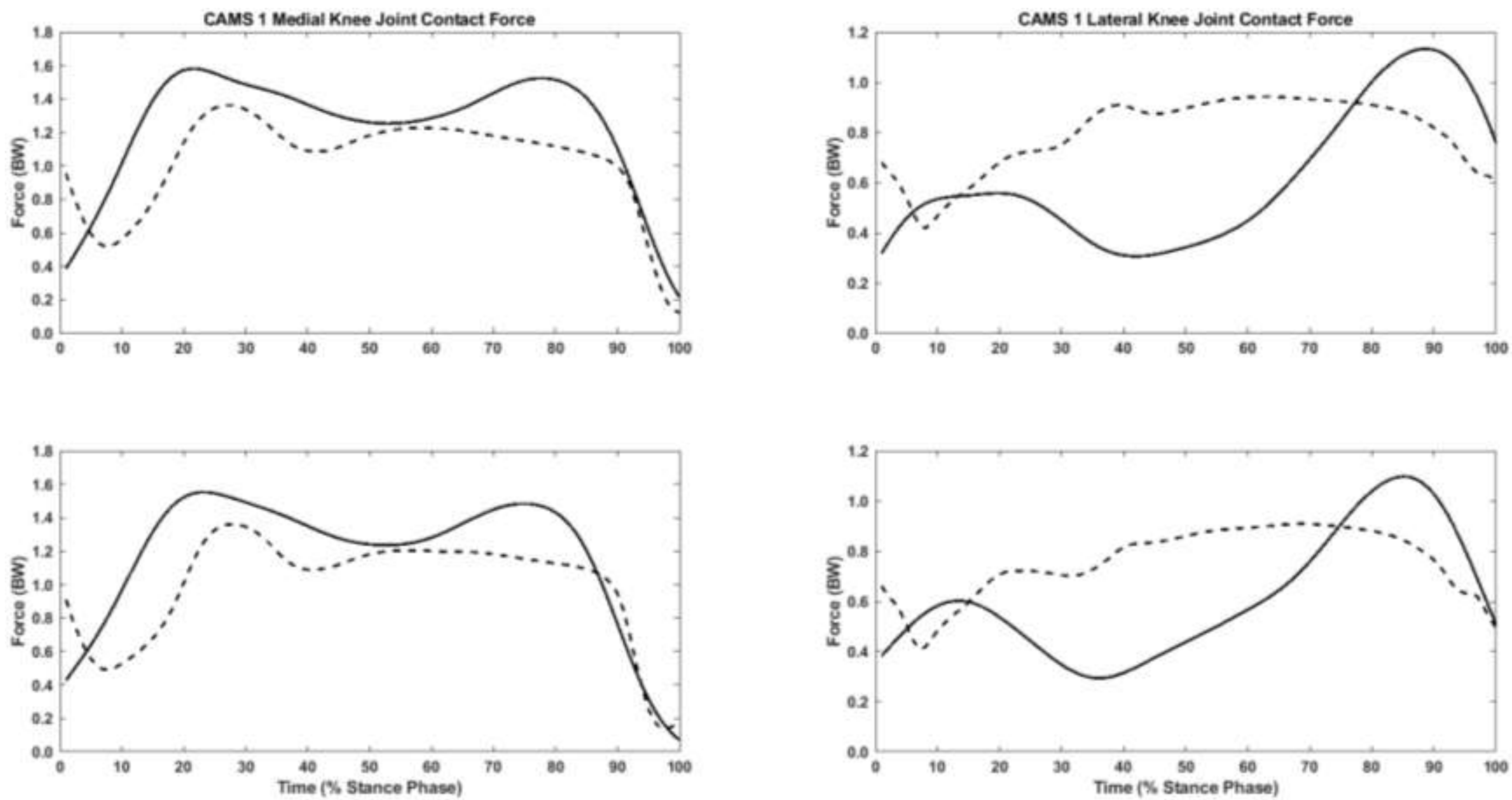

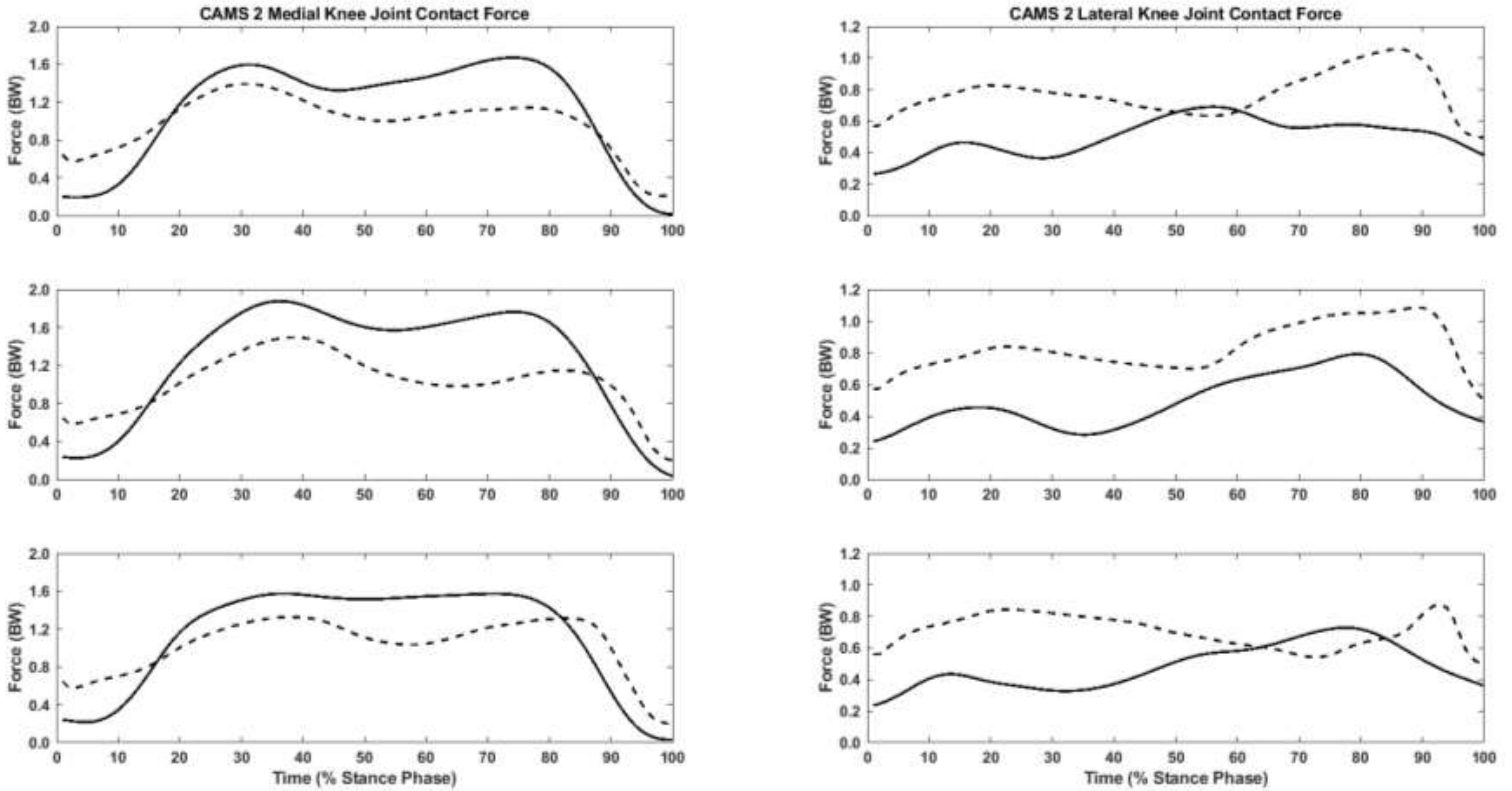

CAMS 2 Medial Knee Joint Contact Force
CAMS 2 Lateral Knee Joint Contact Force
Force (BW)
Time (% Stance Phase)

Appendix Figure 7. Network 3 predictions per trial for each CAMS subject.

Appendix Figure 7 Caption. In-vivo and Network 3 predictions of knee joint contact forces are the solid and dashed lines, respectively.

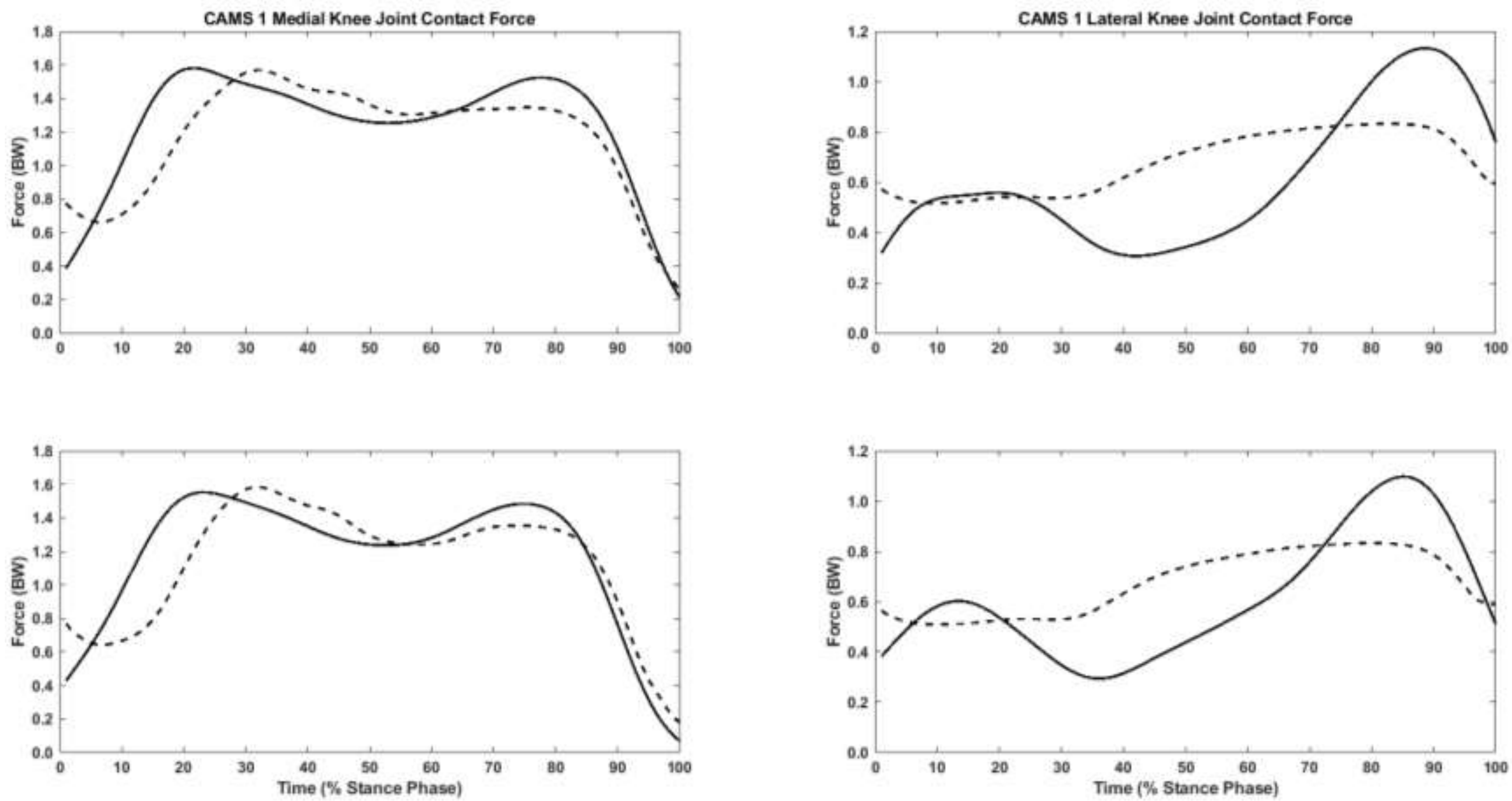

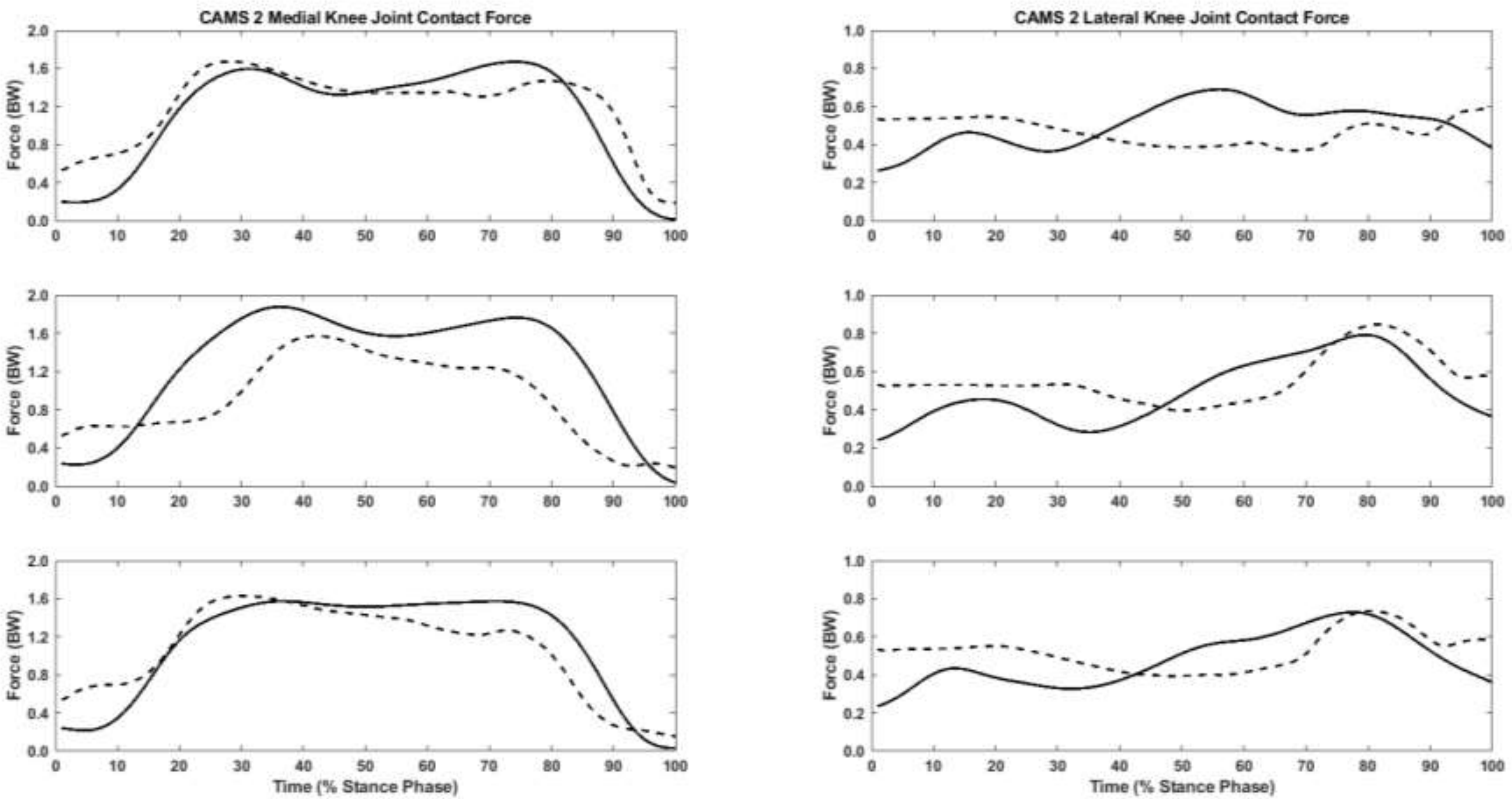
CAMS 2 Medial Knee Joint Contact Force
CAMS 2 Lateral Knee Joint Contact Force
Force (BW)
Time (% Stance Phase)

Appendix Figure 8. Network 4 predictions per trial for each CAMS subject.

Appendix Figure 8 Caption. In-vivo and Network 4 predictions of knee joint contact forces are the solid and dashed lines, respectively.

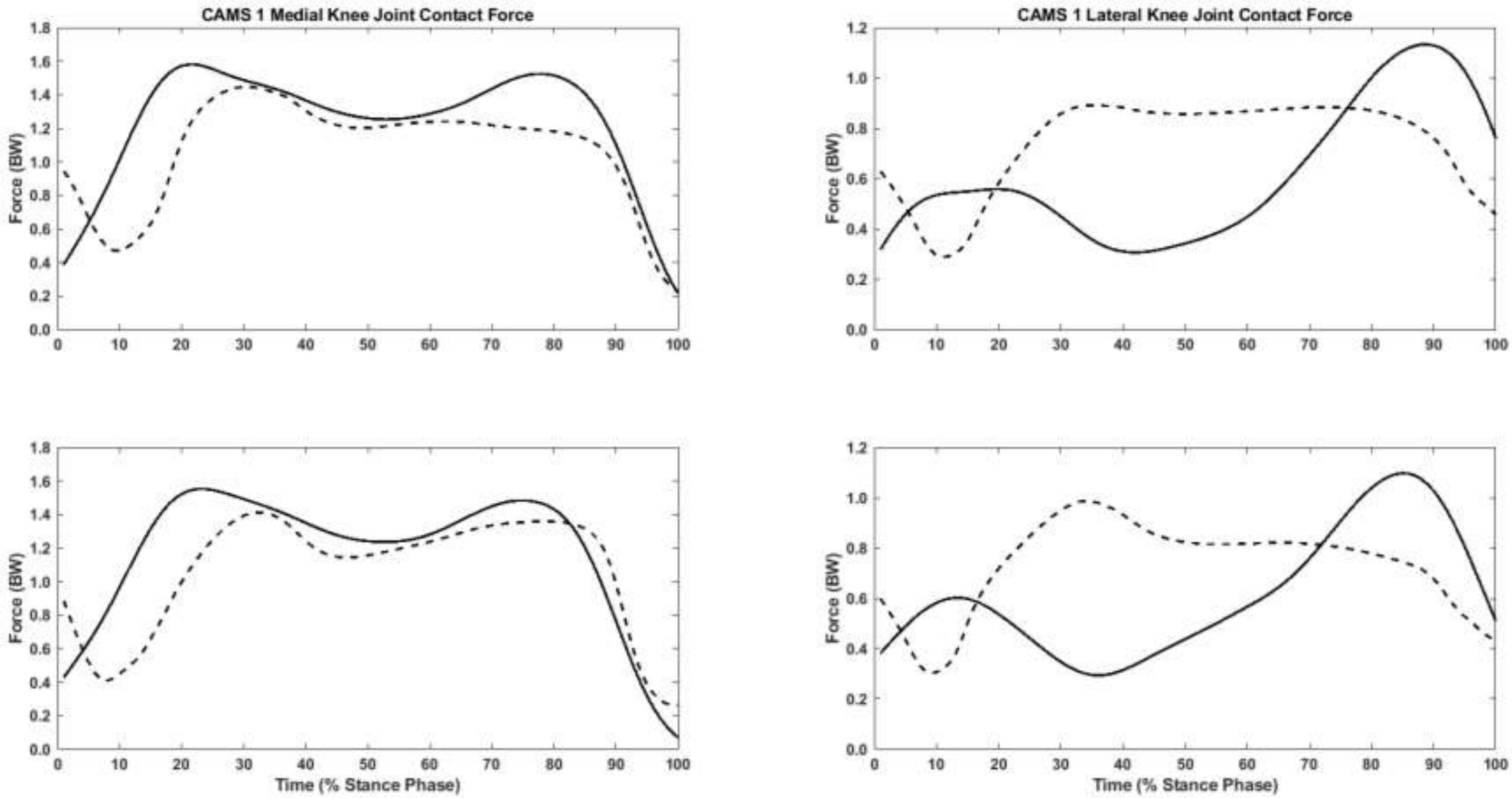

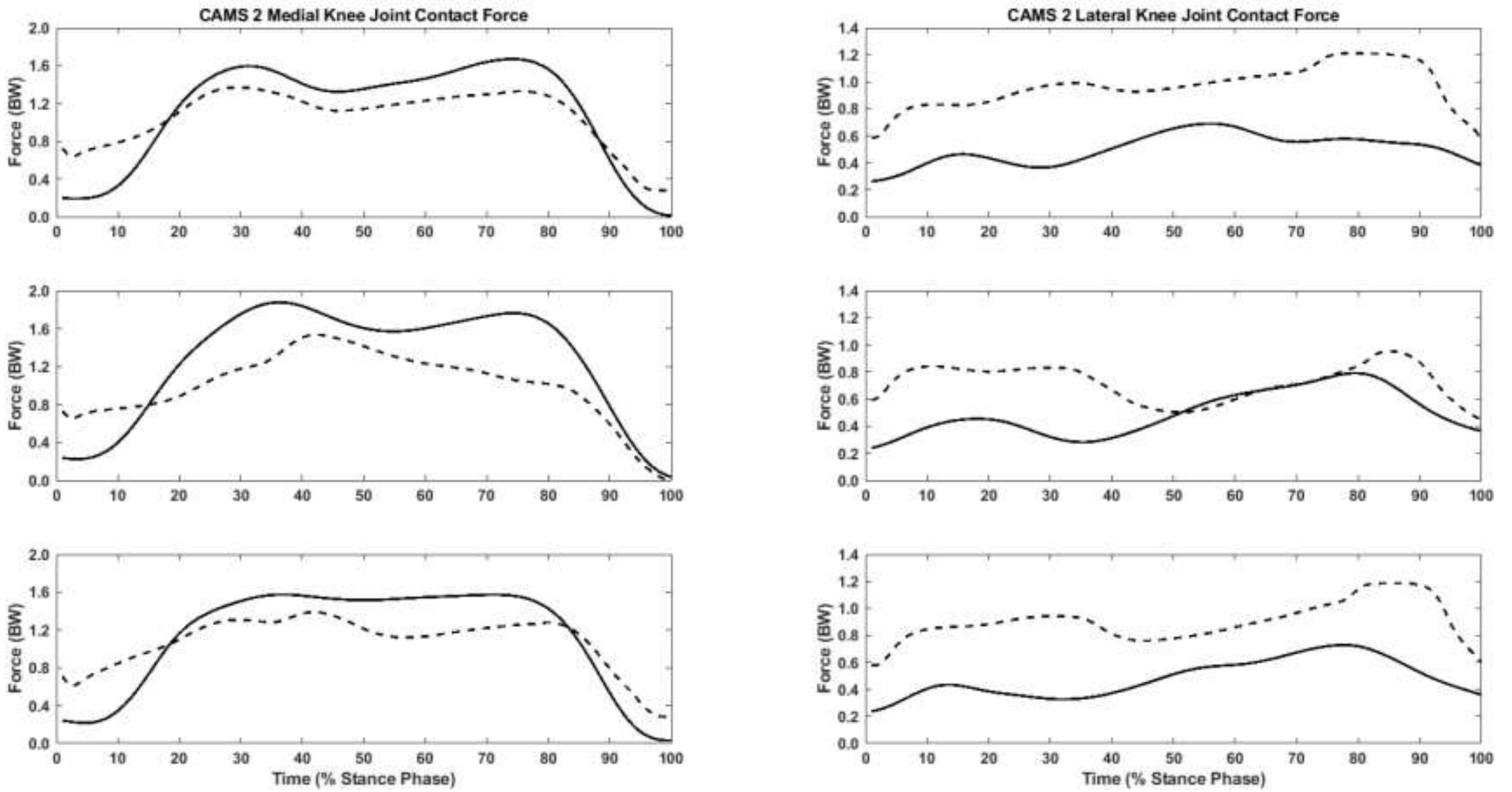
CAMS 2 Medial Knee Joint Contact Force
CAMS 2 Lateral Knee Joint Contact Force
Force (BW)
Time (% Stance Phase)

Appendix Figure 9. Network 5 predictions per trial for each CAMS subject.

Appendix Figure 9 Caption. In-vivo and Network 5 predictions of knee joint contact forces are the solid and dashed lines, respectively.

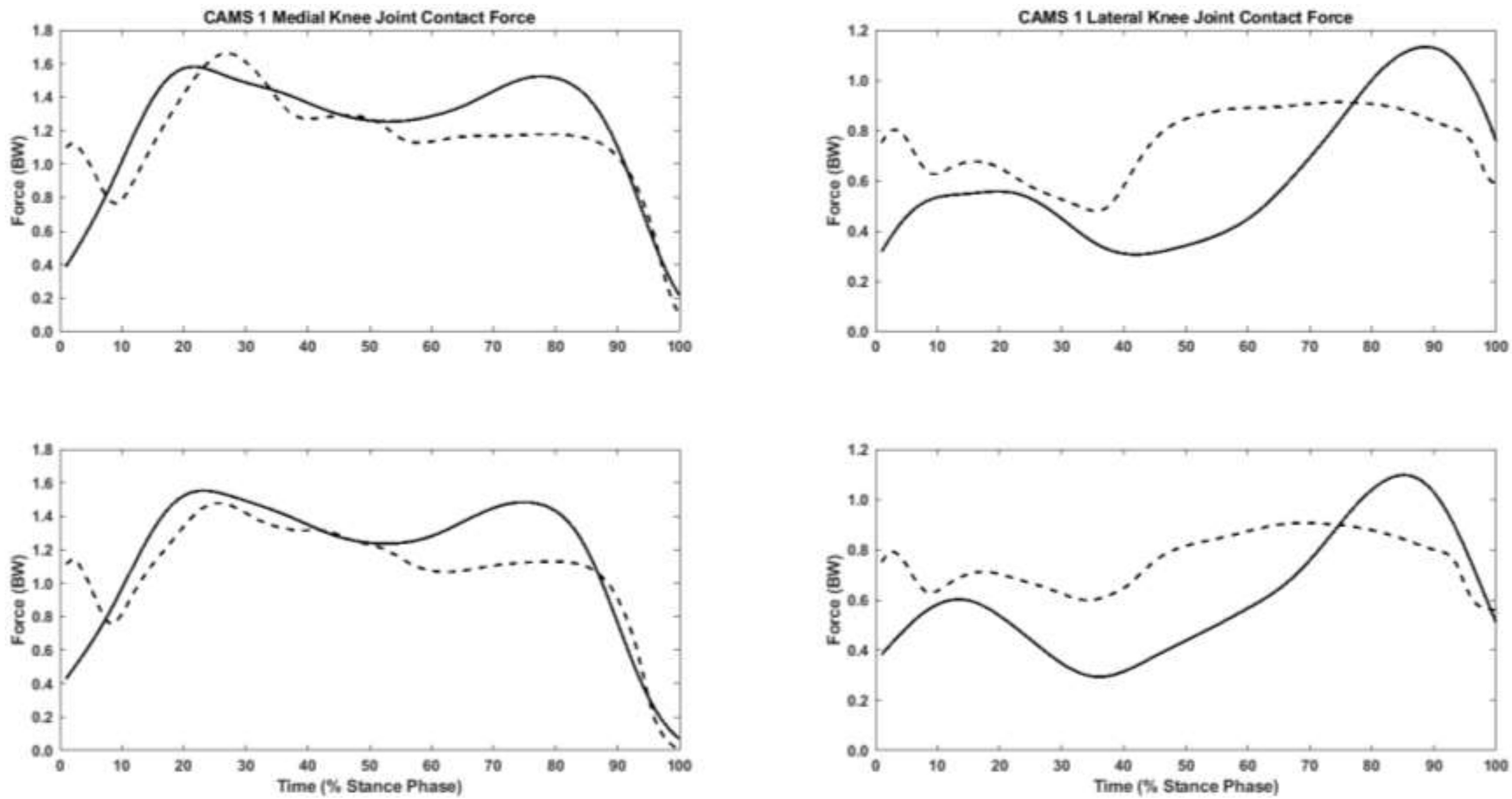

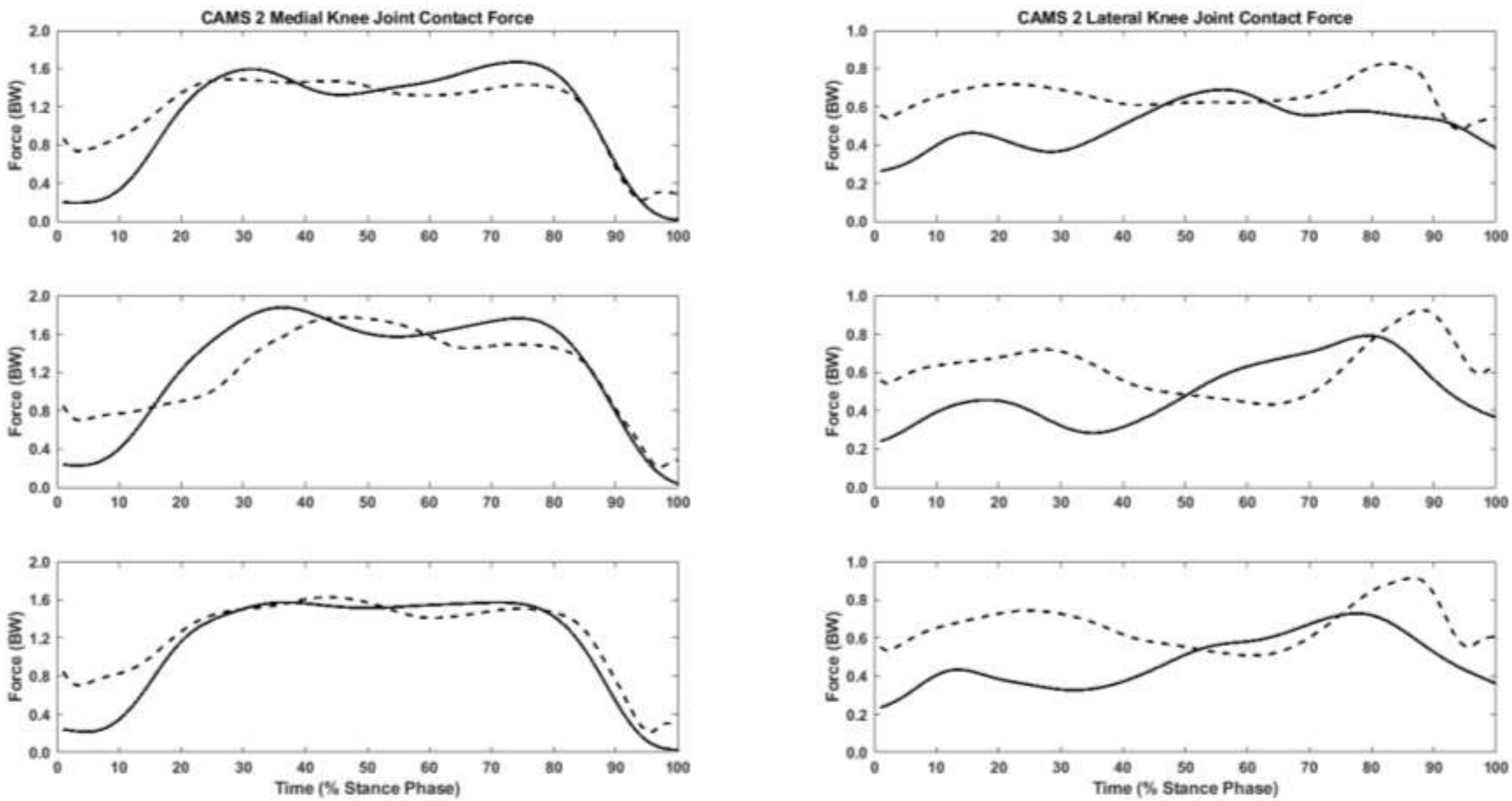
CAMS 2 Medial Knee Joint Contact Force
CAMS 2 Lateral Knee Joint Contact Force
Force (BW)
Time (% Stance Phase)

VITA

Kaileigh Elisabeth Estler

DEPARTMENT
Human Movement Sciences
2016 Student Rec Center
Norfolk, VA 23529

EDUCATION

Present **Masters of Science, Exercise Science, concentration in Biomechanics**
Old Dominion University, Norfolk VA

2019 **Bachelor of Science, Exercise Science**
Old Dominion University, Norfolk VA

PROFESSIONAL EXPERIENCE

2021 ***Old Dominion University, Human Movement Sciences***
GRADUATE TEACHING ASSISTANT, BIOMECHANICS
Supervisor: Dr. Hunter Bennet
Duties and responsibilities include teaching biomechanical research methodologies to all undergraduate biomechanics students, teaching the usage of software used in biomechanics (Vicon Nexus, Visual3D), hold office hours for review of lecture material, and grading of lab projects and presentations

2019-2020 ***Old Dominion University, Neuromechanics Laboratory***
GRADUATE ASSISTANT LAB MANAGER
Supervisor: Dr. Hunter Bennet
Duties and responsibilities include preparation of all lab equipment prior to data collections, assist with laboratory data collections, develop troubleshooting procedures, manage equipment inventory and budget, organize research calendar

LIST OF REFERENCES

Arjmand, N., Ekrami, O., Shirazi-Adl, A., Plamondon, A., & Parnianpour, M. (2013). Relative performances of artificial neural network and regression mapping tools in evaluation of spinal loads and muscle forces during static lifting. *Journal of Biomechanics*, *46*(8), 1454–1462. https://doi.org/10.1016/j.jbiomech.2013.02.026

Astephen, J. L., Deluzio, K. J., Caldwell, G. E., & Dunbar, M. J. (2008). Biomechanical changes at the hip, knee, and ankle joints during gait are associated with knee osteoarthritis severity. *Journal of Orthopaedic Research*, *26*(3), 332–341. https://doi.org/10.1002/jor.20496

Bade, M. J., Kohrt, W. M., & Stevens-Lapsley, J. E. (2010). Outcomes before and after total knee arthroplasty compared to healthy adults. *Journal of Orthopaedic and Sports Physical Therapy*, *40*(9), 559–567. https://doi.org/10.2519/jospt.2010.3317

Bade, M. J., Kohrt, W. M., & Stevens-Lapsley, J. E. (2010). Outcomes before and after total knee arthroplasty compared to healthy adults. *Journal of Orthopaedic and Sports Physical Therapy*, *40*(9), 559–567. https://doi.org/10.2519/jospt.2010.3317

Bennell, K. L., Bowles, K. A., Wang, Y., Cicuttini, F., Davies-Tuck, M., & Hinman, R. S. (2011). Higher dynamic medial knee load predicts greater cartilage loss over 12 months in medial knee osteoarthritis. *Annals of the Rheumatic Diseases*, *70*(10), 1770–1774. https://doi.org/10.1136/ard.2010.147082

Bennett, H. J., Valenzuela, K. A., Lynn, S. K., & Weinhandl, J. T. (2020). Foot Rotation Gait Modifications Affect Hip and Ankle, but Not Knee, Stance Phase Joint Reaction Forces during Running. *Journal of Biomechanical Engineering*, *143*(2). https://doi.org/10.1115/1.4047994

Bennett, H. J., Zhang, S., Shen, G., Weinhandl, J. T., Paquette, M. R., Reinbolt, J., & Coe, D. P. (2017). Effects of Toe-In and Wider Step Width in Stair Ascent with Different Knee Alignments. *Medicine and Science in Sports and Exercise*, *49*(3), 563–572. https://doi.org/10.1249/MSS.0000000000001140

Bourne, R. B., Chesworth, B. M., Davis, A. M., Mahomed, N. N., & Charron, K. D. J. (2010). Patient satisfaction after total knee arthroplasty: Who is satisfied and who is not? *Clinical Orthopaedics and Related Research*, *468*(1), 57–63. https://doi.org/10.1007/s11999-009-1119-9

Boyer, K. A., & Hafer, J. F. (2019). Gait mechanics contribute to exercise induced pain flares in knee osteoarthritis. *BMC Musculoskeletal Disorders*, *20*(1), 1–10. https://doi.org/10.1186/s12891-019-2493-4

Chen, Z., Zhang, X., Ardestani, M. M., Wang, L., Liu, Y., Lian, Q., He, J., Li, D., & Jin, Z. (2014). Prediction of in vivo joint mechanics of an artificial knee implant using rigid multibody dynamics with elastic contacts. *Proceedings of the Institution of Mechanical Engineers, Part H: Journal of Engineering in Medicine*, *228*(6), 564–575. https://doi.org/10.1177/0954411914537476

Creaby, M. W., Wang, Y., Bennell, K. L., Hinman, R. S., Metcalf, B. R., Bowles, K. A., & Cicuttini, F. M. (2010). Dynamic knee loading is related to cartilage defects and tibial plateau bone area in medial knee osteoarthritis. *Osteoarthritis and Cartilage*, *18*(11), 1380–1385. https://doi.org/10.1016/j.joca.2010.08.013

Creaby, M. W., Hunt, M. A., Hinman, R. S., & Bennell, K. L. (2013). Sagittal plane joint loading is related to knee flexion in osteoarthritic gait. *Clinical Biomechanics*, *28*(8), 916–920. https://doi.org/10.1016/j.clinbiomech.2013.07.013

Deepak Kumar, P.T., Ph.D., O.C.S.1, Kurt T. Manal, Ph.D.2, and Katherine S. Rudolph, P.T., P. D. . (2013). Knee Joint Loading during Gait in Healthy Controls and Osteoarthritis. *Osteoarthritis Cartilage*, *21*(2), 298–305. https://doi.org/10.1038/jid.2014.371

Ding, Z., Nolte, D., Tsang, C. K., Cleather, D. J., Kedgley, A. E., & Bull, A. M. J. (2016). In vivo knee contact force prediction using patient-specific musculoskeletal geometry in a segment-based computational model. *Journal of Biomechanical Engineering*, *138*(2), 1–9. https://doi.org/10.1115/1.4032412

D'Lima, D. D., Patil, S., Steklov, N., Slamin, J. E., & Colwell, C. W. (2006). Tibial forces measured in vivo after total knee arthroplasty. *Journal of Arthroplasty*, *21*(2), 255–262. https://doi.org/10.1016/j.arth.2005.07.011

Du, Y., Almajalid, R., Shan, J., & Zhang, M. (2018). A novel method to predict knee osteoarthritis progression on MRY using machine learning methods. *IEEE Transactions on Nanobioscience*, *17*(3).

Du, Y., Shan, J., & Zhang, M. (2017). Knee osteoarthritis prediction on MR images using cartilage damage index and machine learning methods. *Proceedings - 2017 IEEE International Conference on Bioinformatics and Biomedicine, BIBM 2017*, *2017-Janua*, 671–677. https://doi.org/10.1109/BIBM.2017.8217734

Favre, J., Hayoz, M., Erhart-Hledik, J. C., & Andriacchi, T. P. (2012). A neural network model to predict knee adduction moment during walking based on ground reaction force and anthropometric measurements. *Journal of Biomechanics*, *45*(4), 692–698. https://doi.org/10.1016/j.jbiomech.2011.11.057

Felson, D. T. (2009). Developments in the clinical understanding of osteoarthritis. *Arthritis Research and Therapy*, *11*(1). https://doi.org/10.1186/ar2531

Filtjens, B., Nieuwboer, A., D'cruz, N., Spildooren, J., Slaets, P., & Vanrumste, B. (2020). A data-driven approach for detecting gait events during turning in people with Parkinson's disease and freezing of gait. *Gait and Posture*, *80*(May), 130–136. https://doi.org/10.1016/j.gaitpost.2020.05.026

Fragkiadaki, K., Levine, S., Felsen, P., & Malik, J. (2015). Recurrent network models for human dynamics. *Proceedings of the IEEE International Conference on Computer Vision*, *2015 Inter*, 4346–4354. https://doi.org/10.1109/ICCV.2015.494

Geffre, C. P., Bliss, C. L., Szivek, J. A., DeYoung, D. W., Ruth, J. T., & Margolis, D. S. (2008). Sensate scaffolds coupled to telemetry can monitor in vivo loading from within a joint over extended periods of time. *Journal of Biomedical Materials Research - Part B Applied Biomaterials*, *84*(1), 263–270. https://doi.org/10.1002/jbm.b.30869

Gers, F. A., & Schmidhuber, J. (2001). LSTM recurrent networks learn simple context-free and context-sensitive languages. *IEEE Transactions on Neural Networks*, *12*(6), 1333–1340. https://doi.org/10.1109/72.963769

Guo, M., Axe, M. J., & Manal, K. (2007). The influence of foot progression angle on the knee adduction moment during walking and stair climbing in pain free individuals with knee osteoarthritis. *Gait and Posture*, *26*(3), 436–441. https://doi.org/10.1016/j.gaitpost.2006.10.008

Hálfdanardóttir, F., Ramsey, D. K., & Briem, K. (2020). Timing of frontal plane trunk lean, not magnitude, mediates frontal plane knee joint loading in patients with moderate medial knee osteoarthritis. *Advances in Orthopedics*, *2018*(Ic). https://doi.org/10.1155/2018/4526872

Hast, M. W., & Piazza, S. J. (2013). Dual-joint modeling for estimation of total knee replacement contact forces during locomotion. *Journal of Biomechanical Engineering*, *135*(2), 1–9. https://doi.org/10.1115/1.4023320

Heinlein, B., Kutzner, I., Graichen, F., Bender, A., Rohlmann, A., Halder, A. M., Beier, A., & Bergmann, G. (2009). ESB clinical biomechanics award 2008: Complete data of total knee replacement loading for level walking and stair climbing measured in vivo with a follow-up of 6-10 months. *Clinical Biomechanics*, *24*(4), 315–326. https://doi.org/10.1016/j.clinbiomech.2009.01.011

Hochreiter, S., & Schmidhuber, J. (1997). Long Short-Term Memory. *Neural Computation*, *9*(8), 1735–1780. https://doi.org/10.1162/neco.1997.9.8.1735

Holzreiter, S. H., & Köhle, M. E. (1993). Assessment of gait patterns using neural networks. *Journal of Biomechanics*, *26*(6), 645–651. https://doi.org/10.1016/0021-9290(93)90028-D

Hootman, J. M., & Helmick, C. G. (2006). Projections of US prevalence of arthritis and associated activity limitations. *Arthritis and Rheumatism*, *54*(1), 226–229. https://doi.org/10.1002/art.21562

Hunt, M. A., Birmingham, T. B., Giffin, J. R., & Jenkyn, T. R. (2006). Associations among knee adduction moment, frontal plane ground reaction force, and lever arm during walking in patients with knee osteoarthritis. *Journal of Biomechanics*, *39*(12), 2213–2220. https://doi.org/10.1016/j.jbiomech.2005.07.002

Hurwitz, D. E., Ryals, A. B., Case, J. P., Block, J. A., & Andriacchi, T. P. (2002). The knee adduction moment during gait in subjects with knee osteoarthritis is more closely correlated with static alignment than radiographic disease severity, toe out angle and pain. *Journal of Orthopaedic Research*, *20*(1), 101–107. https://doi.org/10.1016/S0736-0266(01)00081-X

Im, S. C., & Kim, K. (2019). Comparison of medial femoral cartilage deformation in normal adults according to gait conditions. *Journal of Exercise Rehabilitation*, *15*(3), 407–413. https://doi.org/10.12965/jer.1938192.096

Judge, A., Arden, N. K., Cooper, C., Kassim javaid, M., Carr, A. J., Field, R. E., & Dieppe, P. A. (2012). Predictors of outcomes of total knee replacement surgery. *Rheumatology (United Kingdom)*, *51*(10), 1804–1813. https://doi.org/10.1093/rheumatology/kes075

Jung, Y., Koo, Y. jun, & Koo, S. (2017). Simultaneous estimation of ground reaction force and knee contact force during walking and squatting. *International Journal of Precision Engineering and Manufacturing*, *18*(9), 1263–1268. https://doi.org/10.1007/s12541-017-0148-7

Jung, Y., Phan, C. B., & Koo, S. (2016). Intra-articular knee contact force estimation during walking using force-reaction elements and subject-specific joint model. *Journal of Biomechanical Engineering*, *138*(2), 1–9. https://doi.org/10.1115/1.4032414

Kaczmarczyk, K., Wit, A., Krawczyk, M., & Zaborski, J. (2009). Gait classification in post-stroke patients using artificial neural networks. *Gait and Posture*, *30*(2), 207–210. https://doi.org/10.1016/j.gaitpost.2009.04.010

Kaufman, K. R., Kovacevic, N., Irby, S. E., & Colwell, C. W. (1996). Instrumented implant for measuring tibiofemoral forces. *Journal of Biomechanics*, *29*(5), 667–671. https://doi.org/10.1016/0021-9290(95)00124-7

Khan, S. S., Khan, S. J., & Usman, J. (2017). Effects of toe-out and toe-in gait with varying walking speeds on knee joint mechanics and lower limb energetics. *Gait and Posture*, *53*, 185–192. https://doi.org/10.1016/j.gaitpost.2017.01.022

Kia, M., Stylianou, A. P., & Guess, T. M. (2014). Evaluation of a musculoskeletal model with prosthetic knee through six experimental gait trials. *Medical Engineering and Physics*, *36*(3), 335–344. https://doi.org/10.1016/j.medengphy.2013.12.007

Kidziński, Ł., Delp, S., & Schwartz, M. (2019). Automatic real-time gait event detection in children using deep neural networks. *PLoS ONE*, *14*(1), 1–11. https://doi.org/10.1371/journal.pone.0211466

Kim, T. K., Chang, C. B., Kang, Y. G., Kim, S. J., & Seong, S. C. (2009). Causes and Predictors of Patient's Dissatisfaction After Uncomplicated Total Knee Arthroplasty. *Journal of Arthroplasty*, *24*(2), 263–271. https://doi.org/10.1016/j.arth.2007.11.005

Kinney, A. L., Besier, T. F., Silder, A., Delp, S. L., D'Lima, D. D., & Fregly, B. J. (2013). Changes in in vivo knee contact forces through gait modification. *Journal of Orthopaedic Research*, *31*(3), 434–440. https://doi.org/10.1002/jor.22240

Kirking, B., Krevolin, J., Townsend, C., Colwell, C. W., & D'Lima, D. D. (2006). A multiaxial force-sensing implantable tibial prosthesis. *Journal of Biomechanics*, *39*(9), 1744–1751. https://doi.org/10.1016/j.jbiomech.2005.05.023

Knarr, B. A., & Higginson, J. S. (2015). Practical approach to subject-specific estimation of knee joint contact force. *Journal of Biomechanics*, *48*(11), 2897–2902. https://doi.org/10.1016/j.jbiomech.2015.04.020

Knarr, B. A., Kesar, T. M., Reisman, D. S., Binder-Macleod, S. A., & Higginson, J. S. (2013). Changes in the activation and function of the ankle plantar flexor muscles due to gait retraining in chronic stroke survivors. *Journal of neuroengineering and rehabilitation*, *10*(1), 1-8.

Ko, Y., Narayanasamy, S., Wee, H. L., Lo, N. N., Yeo, S. J., Yang, K. Y., Yeo, W., Chong, H. C., & Thumboo, J. (2011). Health-related quality of life after total knee replacement or unicompartmental knee arthroplasty in an urban asian population. *Value in Health*, *14*(2), 322–328. https://doi.org/10.1016/j.jval.2010.08.005

Komnik, I., Peters, M., Funken, J., David, S., Weiss, S., & Potthast, W. (2016). Non-sagittal knee joint kinematics and kinetics during gait on level and sloped grounds with unicompartmental and total knee arthroplasty patients. *PLoS ONE*, *11*(12), 1–18. https://doi.org/10.1371/journal.pone.0168566

Kremers, H. M., Larson, D. R., Crowson, C. S., Kremers, W. K., Washington, R. E., Steiner, C. A., Jiranek, W. A., & Berry, D. J. (2014). Prevalence of total hip and knee replacement in the United States. *Journal of Bone and Joint Surgery - American Volume*, *97*(17), 1386–1397. https://doi.org/10.2106/JBJS.N.01141

Kurtz, S. M., Lau, E., Ong, K., Zhao, K., Kelly, M., & Bozic, K. J. (2009). Future young patient demand for primary and revision joint replacement: National projections from 2010 to 2030. *Clinical Orthopaedics and Related Research*, *467*(10), 2606–2612. https://doi.org/10.1007/s11999-009-0834-6

Kutzner, I., Heinlein, B., Graichen, F., Bender, A., Rohlmann, A., Halder, A., Beier, A., & Bergmann, G. (2010). Loading of the knee joint during activities of daily living measured in vivo in five subjects. *Journal of Biomechanics*, *43*(11), 2164–2173. https://doi.org/10.1016/j.jbiomech.2010.03.046

Kutzner, I., Trepczynski, A., Heller, M. O., & Bergmann, G. (2013). Knee adduction moment and medial contact force-facts about their correlation during gait. *PLoS ONE*, *8*(12), 8–15. https://doi.org/10.1371/journal.pone.0081036

Lerner, Z. F., DeMers, M. S., Delp, S. L., & Browning, R. C. (2015). How tibiofemoral alignment and contact locations affect predictions of medial and lateral tibiofemoral contact forces. *Journal of Biomechanics*, *48*(4), 644–650. https://doi.org/10.1016/j.jbiomech.2014.12.049

Liu, Y., Shih, S. M., Tian, S. L., Zhong, Y. J., & Li, L. (2009). Lower extremity joint torque predicted by using artificial neural network during vertical jump. *Journal of Biomechanics*, *42*(7), 906–911. https://doi.org/10.1016/j.jbiomech.2009.01.033

Lundberg, H. J., Knowlton, C., & Wimmer, M. A. (2013). Fine tuning total knee replacement contact force prediction algorithms using blinded model validation. *Journal of Biomechanical Engineering*, *135*(2), 1–9. https://doi.org/10.1115/1.4023388

Luu, T. P., Low, K. H., Qu, X., Lim, H. B., & Hoon, K. H. (2014). An individual-specific gait pattern prediction model based on generalized regression neural networks. *Gait and Posture*, *39*(1), 443–448. https://doi.org/10.1016/j.gaitpost.2013.08.028

Manal, K., & Buchanan, T. S. (2013). An electromyogram-driven musculoskeletal model of the knee to predict in vivo joint contact forces during normal and novel gait patterns. *Journal of Biomechanical Engineering*, *135*(2), 1–7. https://doi.org/10.1115/1.4023457

Marra, M. A., Vanheule, V., Fluit, R., Koopman, B. H. F. J. M., Rasmussen, J., Verdonschot, N., & Andersen, M. S. (2015). A Subject-Specific Musculoskeletal Modeling Framework to Predict in Vivo Mechanics of Total Knee Arthroplasty. *Journal of Biomechanical Engineering*, *137*(2), 1–12. https://doi.org/10.1115/1.4029258

Meireles, S., De Groote, F., Reeves, N. D., Verschueren, S., Maganaris, C., Luyten, F., & Jonkers, I. (2016). Knee contact forces are not altered in early knee osteoarthritis. *Gait and Posture*, *45*, 115–120. https://doi.org/10.1016/j.gaitpost.2016.01.016

Messier, S. P., DeVita, P., Cowan, R. E., Seay, J., Young, H. C., & Marsh, A. P. (2005). Do older adults with knee osteoarthritis place greater loads on the knee during gait? A preliminary study. *Archives of Physical Medicine and Rehabilitation*, *86*(4), 703–709. https://doi.org/10.1016/j.apmr.2004.05.015

Messier, S. P., Pater, M., Beavers, D. P., Legault, C., Loeser, R. F., Hunter, D. J., & DeVita, P. (2014). Influence of alignment and obesity on knee joint loading in osteoarthritic gait. *Osteoarthritis and Cartilage*, *22*(7), 912–917. https://doi.org/10.1016/j.joca.2014.05.013.Influences

Messier, S. P., Pater, M., Beavers, D. P., Legault, C., Loeser, R. F., Huner, D. J., & Devita, P. (2014). Influences of alignment and obesity on knee joint loading in osteoarthritic gait.

Osteoarthritis and Cartilage, *22*(7), 912–917. https://doi.org/10.1016/j.joca.2014.05.013.Influences

Mezghani, N., Husse, S., Boivin, K., Turcot, K., Aissaoui, R., Hagemeister, N., & De Guise, J. A. (2008). Automatic classification of asymptomatic and osteoarthritis knee gait patterns using kinematic data features and the nearest neighbor classifier. *IEEE Transactions on Biomedical Engineering*, *55*(3), 1230–1232. https://doi.org/10.1109/TBME.2007.905388

Mizner, R. L., & Snyder-Mackler, L. (2005). Altered loading during walking and sit-to-stand is affected by quadriceps weakness after total knee arthroplasty. *Journal of Orthopaedic Research*, *23*(5), 1083–1090. https://doi.org/10.1016/j.orthres.2005.01.021

Mündermann, A., Asay, J. L., Mündermann, L., & Andriacchi, T. P. (2008). Implications of increased medio-lateral trunk sway for ambulatory mechanics. *Journal of Biomechanics*, *41*(1), 165–170. https://doi.org/10.1016/j.jbiomech.2007.07.001

Mündermann, A., Dyrby, C. O., & Andriacchi, T. P. (2005). Secondary gait changes in patients with medial compartment knee osteoarthritis: Increased load at the ankle, knee, and hip during walking. *Arthritis and Rheumatism*, *52*(9), 2835–2844. https://doi.org/10.1002/art.21262

Mündermann, A., Dyrby, C. O., D'Lima, D. D., Colwell, C. W., & Andriacchi, T. P. (2008). In vivo knee loading characteristics during activities of daily living as measured by an instrumented total knee replacement. *Journal of Orthopaedic Research*, *26*(9), 1167–1172. https://doi.org/10.1002/jor.20655

Mundt, M., Koeppe, A., Bamer, F., Potthast, W., & Pforzheim, A. C. (2018). Prediction of joint kinetics based on joint kinematics using neural networks. *36th Conference of the International Society of Biomechanics in Sports*, *September*, 794–797. https:/d/sprinz.aut.ac.nz/__data/assets/pdf_file/0012/203106/227_1319_Mundt.pdf%0Ahttps://commons.nmu.edu/isbs/vol36/iss1/190

Mundt, M., Thomsen, W., Witter, T., Koeppe, A., David, S., Bamer, F., Potthast, W., & Markert, B. (2020). Prediction of lower limb joint angles and moments during gait using artificial neural networks. *Medical and Biological Engineering and Computing*, *58*(1), 211–225. https://doi.org/10.1007/s11517-019-02061-3

Nelson, A. E., Fang, F., Arbeeva, L., Cleveland, R. J., Schwartz, T. A., Callahan, L. F., Marron, J. S., & Loeser, R. F. (2019). A machine learning approach to knee osteoarthritis phenotyping: data from the FNIH Biomarkers Consortium. *Osteoarthritis and Cartilage*, *27*(7), 994–1001. https://doi.org/10.1016/j.joca.2018.12.027

Nie, Y., Wang, H., Xu, B., Zhou, Z., Shen, B., & Pei, F. (2019). The Relationship between Knee Adduction Moment and Knee Osteoarthritis Symptoms according to Static Alignment and Pelvic Drop. *BioMed Research International*, *2019*. https://doi.org/10.1155/2019/7603249

Noble, P. C., Conditt, M. A., Cook, K. F., & Mathis, K. B. (2006). The John Insall Award: Patient expectations affect satisfaction with total knee arthroplasty. *Clinical Orthopaedics and Related Research*, *452*, 35–43. https://doi.org/10.1097/01.blo.0000238825.63648.1e

Nüesch, C., Roos, E., Pagenstert, G., & Mündermann, A. (2017). Measuring joint kinematics of treadmill walking and running: Comparison between an inertial sensor based system and a camera-based system. *Journal of Biomechanics*, *57*, 32–38. https://doi.org/10.1016/j.jbiomech.2017.03.015

Oh, S. E., Choi, A., & Mun, J. H. (2013). Prediction of ground reaction forces during gait based on kinematics and a neural network model. *Journal of Biomechanics*, *46*(14), 2372–2380. https://doi.org/10.1016/j.jbiomech.2013.07.036

Paquette, M. R., Klipple, G., & Zhang, S. (2015). Greater step widths reduce internal knee abduction moments in medial compartment knee osteoarthritis patients during stair ascent. *Journal of Applied Biomechanics, 31*(4), 229–236. https://doi.org/10.1123/jab.2014-0166

Rasnick, R., Standifird, T., Reinbolt, J. A., Cates, H. E., & Zhang, S. (2016). Knee joint loads and surrounding muscle forces during stair ascent in patients with total knee replacement. *PLoS ONE, 11*(6), 1–14. https://doi.org/10.1371/journal.pone.0156282

Richards, R. E., Andersen, M. S., Harlaar, J., & van den Noort, J. C. (2018). Relationship between knee joint contact forces and external knee joint moments in patients with medial knee osteoarthritis: effects of gait modifications. *Osteoarthritis and Cartilage*, *26*(9), 1203–1214. https://doi.org/10.1016/j.joca.2018.04.011

Sasaki, K., & Neptune, R. R. (2010). Individual muscle contributions to the axial knee joint contact force during normal walking. *Journal of Biomechanics, 43*(14), 2780–2784. https://doi.org/10.1016/j.jbiomech.2010.06.011

Shull, P. B., Shultz, R., Silder, A., Dragoo, J. L., Besier, T. F., Cutkosky, M. R., & Delp, S. L. (2013). Toe-in gait reduces the first peak knee adduction moment in patients with medial compartment knee osteoarthritis. *Journal of Biomechanics*, *46*(1), 122–128. https://doi.org/10.1016/j.jbiomech.2012.10.019

Simic, M., Wrigley, T. V., Hinman, R. S., Hunt, M. A., & Bennell, K. L. (2013). Altering foot progression angle in people with medial knee osteoarthritis: The effects of varying toe-in and toe-out angles aremediated by pain and malalignment. *Osteoarthritis and Cartilage*, *21*(9), 1272–1280. https://doi.org/10.1016/j.joca.2013.06.001

Smith, A. J., Lloyd, D. G., & Wood, D. J. (2004). Pre-surgery knee joint loading patterns during walking predict the presence and severity of anterior knee pain after total knee arthroplasty. *Journal of Orthopaedic Research*, *22*(2), 260–266. https://doi.org/10.1016/S0736-0266(03)00184-0

Smith, C. R., Vignos, M. F., Lenhart, R. L., Kaiser, J., & Thelen, D. G. (2016). The influence of component alignment and ligament properties on tibiofemoral contact forces in total knee replacement. *Journal of Biomechanical Engineering*, *138*(2). https://doi.org/10.1115/1.4032464

Smith, S. M., Cockburn, R. A., Hemmerich, A., Li, R. M., & Wyss, U. P. (2008). Tibiofemoral joint contact forces and knee kinematics during squatting. *Gait and Posture*, *27*(3), 376–386. https://doi.org/10.1016/j.gaitpost.2007.05.004

Sparkes, V., Whatling, G. M., Biggs, P., Khatib, N., Al-Amri, M., Williams, D., Hemming, R., Hagen, M., Saleem, I., Swaminathan, R., & Holt, C. (2019). Comparison of gait, functional activities, and patient-reported outcome measures in patients with knee osteoarthritis and healthy adults using 3D motion analysis and activity monitoring: An exploratory case-control analysis. *Orthopedic Research and Reviews*, *11*, 129–140. https://doi.org/10.2147/ORR.S199107

Szivek, J. A., Bliss, C. L., Geffre, C. P., Margolis, D. S., DeYoung, D. W., Ruth, J. T., Schnepp, A. B., Tellis, B. C., & Vaidyanathan, R. K. (2006). An instrumented scaffold can monitor loading in the knee joint. *Journal of Biomedical Materials Research - Part B Applied Biomaterials*, *79*(2), 218–228. https://doi.org/10.1002/jbm.b.30532

Teng, H. L., & Powers, C. M. (2014). Sagittal plane trunk posture influences patellofemoral joint stress during running. *Journal of Orthopaedic and Sports Physical Therapy*, *44*(10), 785–792. https://doi.org/10.2519/jospt.2014.5249

Turcot, K., Armand, S., Lübbeke, A., Fritschy, D., Hoffmeyer, P., & Suvà, D. (2013). Does knee alignment influence gait in patients with severe knee osteoarthritis? *Clinical Biomechanics*, *28*(1), 34–39. https://doi.org/10.1016/j.clinbiomech.2012.09.004

Van Den Noort, J. C., Schaffers, I., Snijders, J., & Harlaar, J. (2013). The effectiveness of voluntary modifications of gait pattern to reduce the knee adduction moment. *Human Movement Science*, *32*(3), 412–424. https://doi.org/10.1016/j.humov.2012.02.009

Van Egmond, N., Stolwijk, N., van Heerwaarden, R., van Kampen, A., & Keijsers, N. L. W. (2017). Gait analysis before and after corrective osteotomy in patients with knee osteoarthritis and a valgus deformity. *Knee Surgery, Sports Traumatology, Arthroscopy*, *25*(9), 2904–2913. https://doi.org/10.1007/s00167-016-4045-x

Vissers, M. M., De Groot, I. B., Reijman, M., Bussmann, J. B., Stam, H. J., & Verhaar, J. A. N. (2010). Functional capacity and actual daily activity do not contribute to patient satisfaction after total knee arthroplasty. *BMC Musculoskeletal Disorders*, *11*. https://doi.org/10.1186/1471-2474-11-121

Walter, J. P., D'Lima, D. D., Colwell, C. W., & Fregly, B. J. (2010). Decreased knee adduction moment does not guarantee decreased medial contact force during gait. *Journal of Orthopaedic Research*, *28*(10), 1348–1354. https://doi.org/10.1002/jor.21142

Weinstein, A. M., Rome, B. N., Reichmann, W. M., Collins, J. E., Burbine, S. A., Thornhill, T. S., Wright, J., Katz, J. N., & Losina, E. (2013). Estimating the burden of total knee replacement in the United States. *Journal of Bone and Joint Surgery - Series A*, *95*(5), 385–392. https://doi.org/10.2106/JBJS.L.00206

Weiss, J. M., Noble, P. C., Conditt, M. A., Kohl, H. W., Roberts, S., Cook, K. F., Gordon, M. J., & Mathis, K. B. (2002). What functional activities are important to patients with knee replacements? *Clinical Orthopaedics and Related Research*, *404*, 172–188. https://doi.org/10.1097/01.blo.0000036536.46246.d9

Zeng, W., Liu, F., Wang, Q., Wang, Y., Ma, L., & Zhang, Y. (2016). Parkinson's disease classification using gait analysis via deterministic learning. *Neuroscience Letters*, *633*, 268–278. https://doi.org/10.1016/j.neulet.2016.09.043

Zhao, D., Banks, S. A., D'Lima, D. D., Colwell Jr., C. W., & Fregly, B. J. (2007). In vivo medial and lateral tibial loads during dynamic and high flexion activities. *Journal of Orthopaedic Research September*, *25*(June), 1121–1127. https://doi.org/10.1002/jor

Zhao, D., Banks, S. A., Mitchell, K. H., D'Lima, D. D., Colwell Jr., C. W., & Fregly, B. J. (2007). Correlation between the knee adduction torque and medial contact force for a variety of gait patterns. *Journal of Orthopaedic Research September*, *25*(June), 789–796. https://doi.org/10.1002/jor